Coordination Chemistry Reviews, 39 (1981) 31–75
Elsevier Scientific Publishing Company, Amsterdam—Printed in The Netherlands

STRUCTURAL ASPECTS AND COORDINATION CHEMISTRY OF METAL PORPHYRIN COMPLEXES WITH EMPHASIS ON AXIAL LIGAND BINDING TO CARBON DONORS AND MONO- AND DIATOMIC NITROGEN AND OXYGEN DONORS

P.D. SMITH, B.R. JAMES and D.H. DOLPHIN

Department of Chemistry, University of British Columbia, Vancouver, B.C., V6T 1Y6 (Canada)

(First received 30 October 1980; in revised form 5 January 1981)

CONTENTS

A. Introduction 32
B. Nomenclature 33
C. Metal–carbon bonding 33
(i) Carbonyl complexes 33
(ii) Thiocarbonyl complexes 41
(iii) Carbene complexes 42
(iv) Metal–carbon σ-bonded complexes 43
D. Metal–nitrogen bonding 46
(i) Dinitrogen complexes 46
(ii) Nitrosyl complexes 49
(iii) Nitrido complexes 55
E. Metal–oxygen bonding 56
(i) Coordinated dioxygen: superoxide and peroxide structures 57
(ii) Oxo complexes 61
(iii) Biological implications 63
F. The μ-linked dimers 64
G. Metal–metal bonding 69
Acknowledgements 70
References 70

ABBREVIATIONS

Me	Methyl
Et	Ethyl
Ph	Phenyl
Bu	Butyl
Pr	Propyl
Tol	Tolyl
AcO	Acetate

0010-8545/81/0000–0000/$11.25 © 1981 Elsevier Scientific Publishing Company

Py	Pyridine
THF	Tetrahedrofuran
*N*Me-Im	*N*-Methylimidazole
4Me-Pip	4-Methylpiperidine
DMSO	Dimethyl sulfoxide
P	Porphyrin

A. INTRODUCTION

Porphyrin coordination chemistry has been the subject of several recent reviews [1]. The porphyrin macrocycle has proven to be a very versatile ligand which forms complexes with all the transition metals, many of the main group and several of the rare earth elements. Once chelation has occurred, many of the metalloporphyrins exhibit additional ligand binding to the axial coordination sites above and below the porphyrin plane. Some of the more traditional porphyrin coordination geometries are illustrated in Fig. 1.

In recent years there has been a surge of interest in the coordination chemistry of metalloporphyrins containing small gas molecules as axial

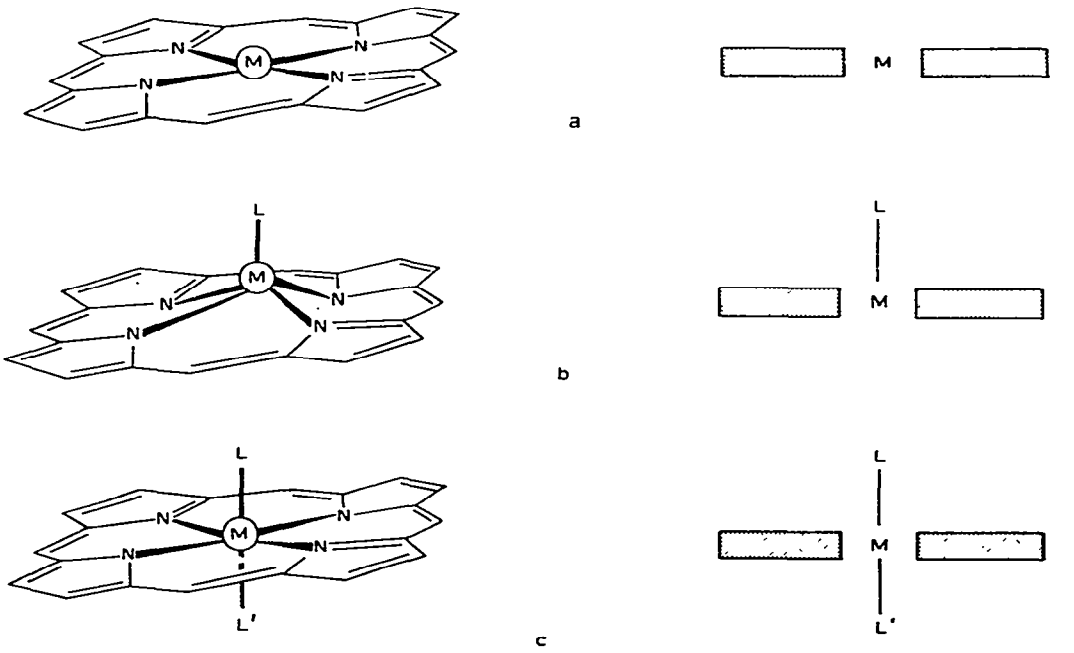

Fig. 1. Common porphyrin coordination geometries, (a) square planar, (b) square pyrimidal and (c) octahedral.

ligands, for example O_2, NO, CO and N_2. The first three mentioned gases are known to react for example with iron(II) porphyrin centers within proteins (myoglobin, hemoglobin) [2] while activation of coordinated O_2 by oxygenases and oxidases, some of them being metalloporphyrin systems, adds particular interest to this gas molecule [3]; a major goal of porphyrin research is to provide model systems for study of the protein systems. The potential of multicenter metalloporphyrins to act as electron transfer reagents in, for example, the four-electron reduction of O_2 to H_2O (fuel cells) and the six-electron reduction of N_2 to NH_3 (nitrogen fixation) is also well recognized [4]. The feature of metal–carbon bonding in the vitamin B_{12} coenzyme [3] sustains interest in organometallic chemistry of metalloporphyrins, as does the more recent suggestion of roles for iron–carbene intermediates within cytochrome P450 enzymes [5].

In this article, we wish to report principally on the axial coordination chemistry of metal–carbon, metal–nitrogen, metal–oxygen and metal–metal bonds of porphyrin complexes in the light of the general topics noted above, which reflect also some of the current research interests in our laboratories. We have emphasized especially X-ray structural data, since we have found this exercise valuable in showing the wide range of geometries now documented for the porphyrin-encircled metal. The often novel geometries should provide further insight into the types of intermediates important in the vast and fascinating chemistry of metalloporphyrins [1].

B. NOMENCLATURE

The various porphyrins mentioned in the text are listed in Table 1 showing the peripheral substituents and the corresponding abbreviations.

C. METAL–CARBON BONDING

(i) Carbonyl complexes

Several examples of monocarbonyl derivatives of metalloporphyrins are listed in Table 2.

The square pyramidal geometry is exemplified by Fe(TPP)CO [6], Fe(Deut)CO [9] and Co(TPP)CO [7]. Exposing solutions of the square planar iron(II) porphyrins in non-coordinating organic solvents to varying partial pressures of carbon monoxide results in the equilibrium

$$\mathrm{Fe(P)} \overset{K_1}{\rightleftharpoons} \mathrm{Fe(P)(CO)} \overset{K_2}{\rightleftharpoons} \mathrm{Fe(P)(CO)_2} \qquad (1)$$

The dicarbonyl derivatives will be discussed below. Equilibrium constants of $K_1 = 6.6 \times 10^4$ and 2×10^4 M^{-1}, $K_2 = 140$ and 200 M^{-1} were reported for

TABLE 1
Relevant porphyrin structures and nomenclature

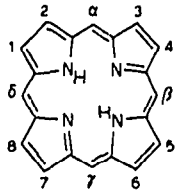

Abbreviation	Name	Substituents [a]								
		1	2	3	4	5	6	7	8	α
OEP	Octaethylporphyrin	Et	Et	Et	Et	Et	Et	Et	Et	H
TPP	Tetraphenylporphyrin	H	H	H	H	H	H	H	H	Ph
TTP	Tetratolylporphyrin	H	H	H	H	H	H	H	H	Tol
Etio-I	Etioporphyrin-I	Me	Et	Me	Et	Me	Et	Me	Et	H
Deut	Deuteroporphyrin	Me	H	Me	H	Me	P^H	P^H	Me	H
Meso IX-DME	Mesoporphyrin IX-dimethylester	Me	Et	Me	Et	Me	P^M	P^M	Me	H
Proto IX	Protoporphyrin IX	Me	V	Me	V	Me	P^H	P^H	Me	H
Proto IX-DME	Protoporphyrin IX-dimethylester	Me	V	Me	V	Me	P^M	P^M	Me	H
OMBP	Octamethyltetrabenzporphyrin	*P*-Xyl		*P*-Xyl		*P*-Xyl		*P*-Xyl		H

[a] Me=methyl; Et=ethyl; Ph=phenyl; $P^M = -CH_2CH_2COOCH_3$; V=vinyl; $P^H = -CH_2CH_2COOH$; *P*-Xyl represents a fused *para*-xylene to the pyrrole rings, $\alpha=\beta=\gamma=\delta$.

TABLE 2
Examples of porphyrin mono-carbonyl complexes

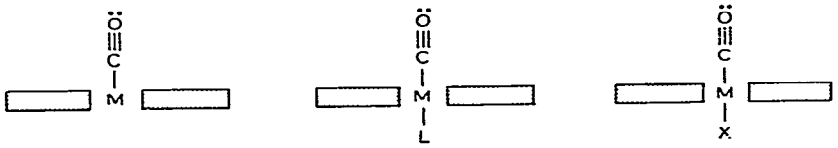

M	P	L	X	Ref.
Fe	TPP			6
Fe	Deut			9
Co	TPP			7
Fe	Proto IX-DME	Py		17
Fe	TPP	Py		29
Ru	Etio-I	Py		10
Ru	OEP	Py		10,11
Ru	TPP	Py		12,14
Ru	TPP	EtOH		15
Os	OEP	Py		16
Co	TPP	O_2 [a]		7
Rh	TPP		Cl	27
Ir	OEP		Cl	28

[a] Spectroscopically characterized at −150°C.

the tetraphenylporphyrin and deuteroporphyrin derivatives, respectively [9].

The monocarbonyl cobalt complex Co(TPP)CO [7] has been identified spectroscopically at −150°C. The instability of this complex can be related to the $(d_{xz}, d_{yz}, d_{xy})^6(d_{z^2})^1$ configuration of cobalt since the single occupancy of the d_{z^2} orbital weakens the cobalt–carbonyl sigma interaction.

The octahedral coordination of divalent metalloporphyrins is illustrated well by the Fe, Ru and Os derivatives listed in Table 2. The affinity for a sixth ligand is so great in the Ru and Os complexes that penta-coordinate monocarbonyl derivatives similar to the Fe(II) complexes have not been observed. Generally speaking, strong field ligands such as pyridine form the more kinetically stable complexes in the series [8,18,25]. The IR-stretching frequency of the carbonyl ligand is quite sensitive to the π-acceptor properties of the *trans* ligand. For example, ν(CO) has been observed to vary between 1858 cm^{-1} and 1968 cm^{-1} for a series of ligands in the complexes Os(OEP)CO(L) [25]. In addition, the CO stretching frequency has been shown to decrease along the series Fe(OEP)CO(Py) > Ru(OEP)CO(Py) > Os(OEP)CO(Py) (ν(CO) = 1967, 1925 and 1902 cm^{-1}, respectively) [25] as backbonding between metal and carbonyl ligand increases.

The crystal structures of Fe(TPP)CO(Py) [29], Ru(TPP)CO(Py) [13] and

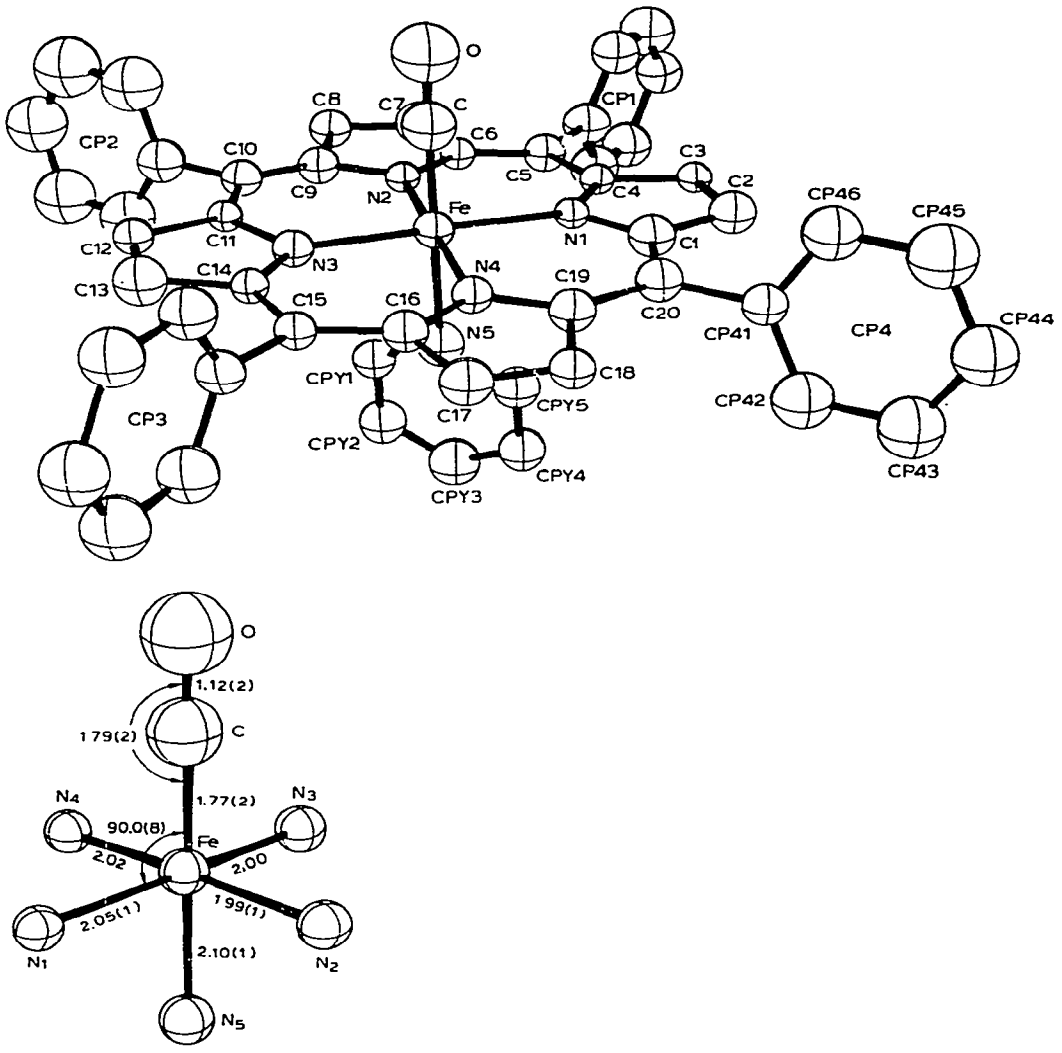

Fig. 2. Computer drawing of the molecule Fe(TPP)CO(Py) and representation of the inner coordination sphere from ref. 29.

Ru(TPP)CO(EtOH) [15] along with selected molecular parameters are shown in Figs. 2, 3 and 4, respectively. Several structural features are worthy of comparison. The metal ion is displaced 0.02 and 0.079 Å from the porphyrin plane toward the carbonyl ligand in Fe(TPP)CO(Py) and Ru(TPP)CO(Py), respectively. The stronger *trans* influence of the pyridine ligand relative to the ethanol ligand in Ru(TPP)CO(Py) and Ru(TPP)CO(EtOH), respectively, is evidenced by the longer metal–carbonyl bond distances in the former (1.84 vs. 1.77 Å). Notably the metal–C–O bond angle is essentially linear in

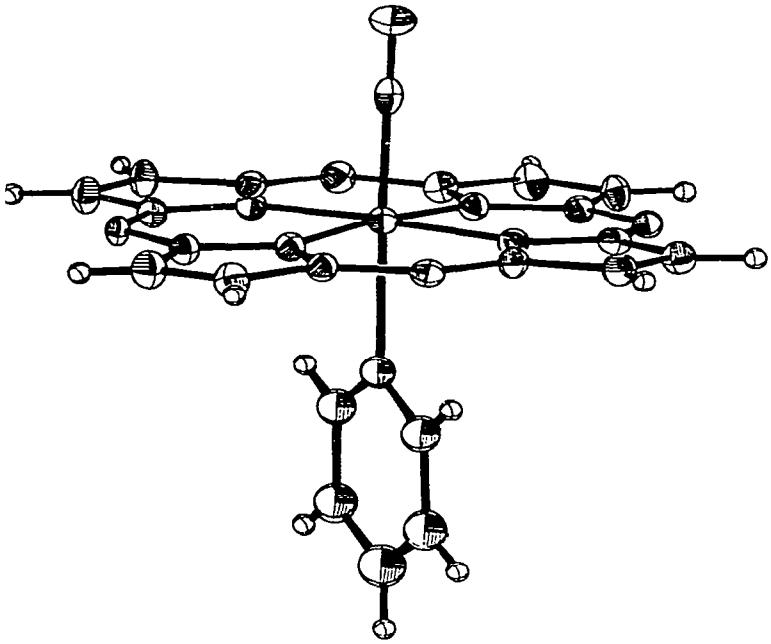

Fig. 3. Computer drawing of the molecule Ru(TPP)CO(Py) from ref. 13.

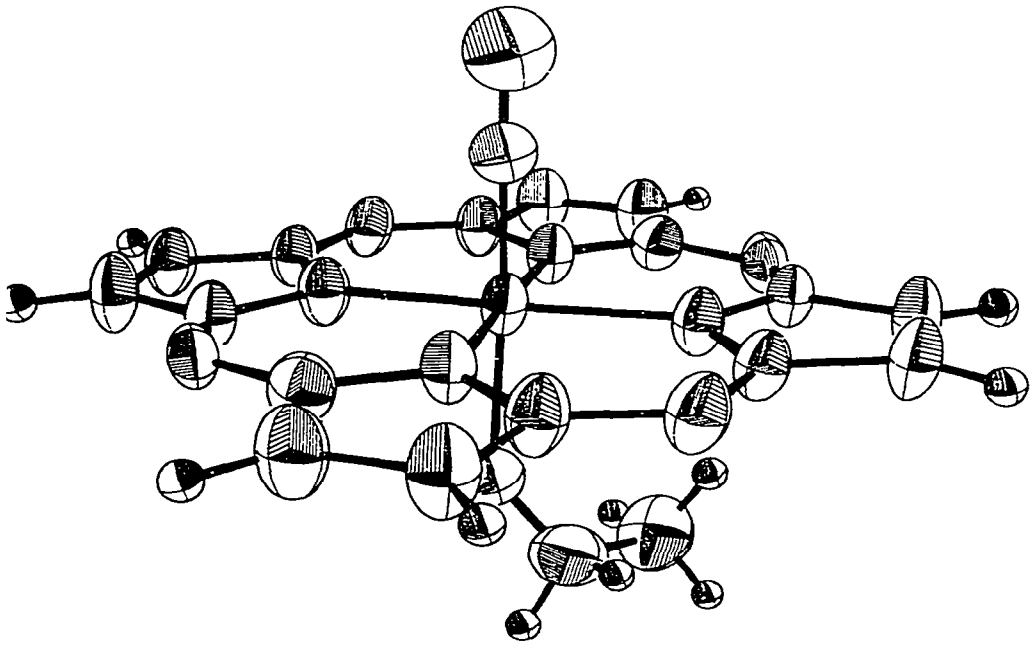

Fig. 4. Computer drawing of the molecule Ru(TPP)CO(EtOH) from ref. 15.

all three structures (179, 178.4 and 175.8° for Fe(TPP)CO(Py), Ru(TPP)CO(Py) and Ru(TPP)CO(EtOH), respectively). In view of this and other data of model compounds [19], the "bent" or "tilted" geometry reported for the CO ligand in several carbonyl hemoproteins [20–24] has usually been attributed to steric constraints placed on the porphyrin coordination sphere by the surrounding protein, although the latest structural data [24] suggest that interactions with the closest atoms (of His-E7 and Val-E11) are not sufficient to tilt a linear Fe–C–O–moiety.

Two other examples of monocarbonyl metalloporphyrins are Rh(TPP)CO(Cl) [27] and Ir(OEP)CO(Cl) [28]. Like the iron(II), ruthenium(II) and osmium(II) complexes mentioned above, the rhodium(III) and iridium(III) compounds have pseudo-octahedral geometry with a low-spin d^6 electronic configuration. The axial site *trans* to the carbonyl ligand is, in these cases, occupied by a chloride ion. Due to the higher oxidation state of the metal ion, the extent of metal–carbonyl backbonding is significantly reduced relative to the divalent ruthenium and osmium carbonyl complexes. The high carbonyl stretching frequency of the rhodium complex (2100 cm^{-1}) is consistent with observed nucleophilic attack by ethoxide ion at the coordinated carbonyl ligand to yield the ethoxycarbonyl rhodium(III) complex Rh(TPP)COOEt [27].

Several examples of monometallic dicarbonyl porphyrin complexes are shown in Table 3. The *trans* configuration is represented by the complexes of divalent iron, ruthenium and osmium. The strong *trans* influence of the

TABLE 3
Examples of porphyrin dicarbonyl complexes

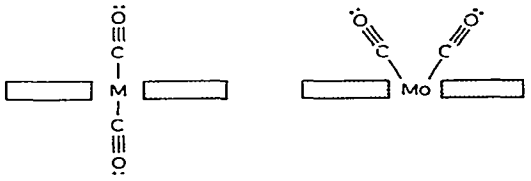

M	P	Ref.
Fe	TPP	6
Fe	Deut	9
Ru	TPP	8
Ru	OEP	8
Os	OEP	25
Mo	TPP [a]	26

[a] ν(CO) = 1940 and 1850 cm^{-1} suggest the *cis* configuration of CO ligands.

opposing carbonyl ligand is evidenced by the extreme lability of one carbonyl ligand toward substitution by other ligands such as H_2O, MeOH, etc. The low values of K_2 reported [6,9] for the reaction

$$Fe(P)CO \overset{K_2}{\rightleftharpoons} Fe(P)(CO)_2 \qquad (2)$$

are also indicative of the thermodynamic instability of the *trans* configuration of carbonyl ligands.

The dicarbonyl complex of molybdenum, $Mo(TPP)(CO)_2$ [26], has two carbonyl stretching frequencies at 1940 and 1850 cm^{-1}, suggesting a *cis* configuration for the carbonyl ligands. The *cis* configuration of axial ligands in divalent molybdenum porphyrins appears to be a preferred arrangement and is displayed by nitrosyl complexes to be discussed later.

In addition to the mono- and dicarbonyl metalloporphyrin derivatives already mentioned, there are several well characterized polycarbonyl complexes. These compounds contain one or two monovalent metal ions coordinated by two or three carbonyl ligands and two or three of the porphyrin nitrogens.

The proposed structure for the complexes $[Re(CO)_3]H$(Meso IX-DME) [30–32], $[Re(CO)_3]H$(TPP) [33] and $[Tc(CO)_3]H$(Meso IX-DME) [31] is shown in Fig. 5. In this structure the $[M(CO)_3]^+$ fragment is coordinated between three porphyrin nitrogens with the proton bound to the remaining nitrogen. The ^1H NMR spectra of both the Re and Tc monometallic complexes indicate fluxional character attributed to intramolecular re-

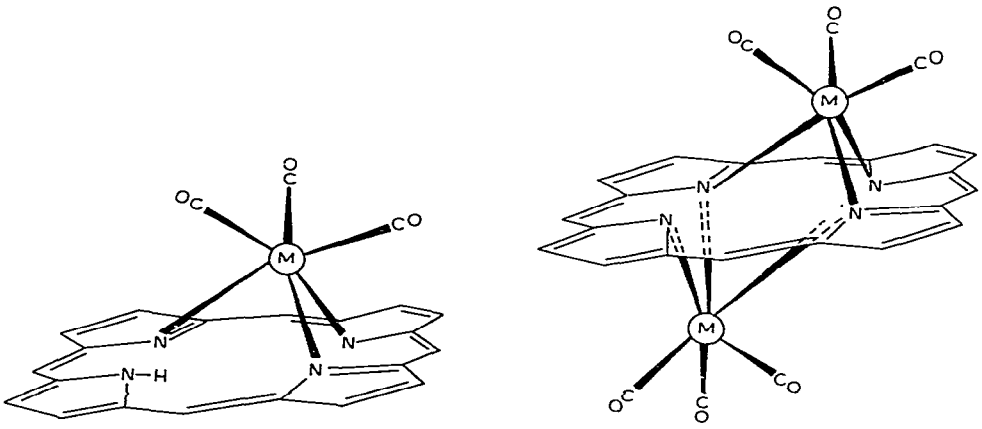

Fig. 5. Proposed structure for the complexes $[Re(CO)_3]H$(Meso IX-DME), $[Re(CO)_3]H$(TPP) and $[Tc(CO)_3]H$(Meso IX-DME).

Fig. 6. Structure of $[Re(CO)_3]_2$(TPP) and $[Tc(CO)_3]_2$(TPP).

arrangement of the $[M(CO)_3]^+$ among the four porphyrin nitrogens with concomitant movement of the N–H proton [34].

A schematic representation of the bimetallic derivatives, $[M(CO)_3]_2(P)$ [35], is shown in Fig. 6 which corresponds to the X-ray structures of $[Re(CO)_3]_2(TPP)$ [33] and $[Tc(CO)_3]_2(TPP)$ [33]. In this structure the porphyrin acts as a hexadentate ligand, coordinating the two $[M(CO)_3]^+$ fragments, one above and one below the porphyrin plane, in such a way that each fragment is coordinated to three porphyrin nitrogens, thus creating a pseudo-octahedral geometry for the monovalent metal ions, Re^+ and Tc^+.

Although the stoichiometry of the bimetallic iridium complex, $[Ir(CO)_3]_2(OEP)$ [28], is identical to the bimetallic complexes of rhenium and

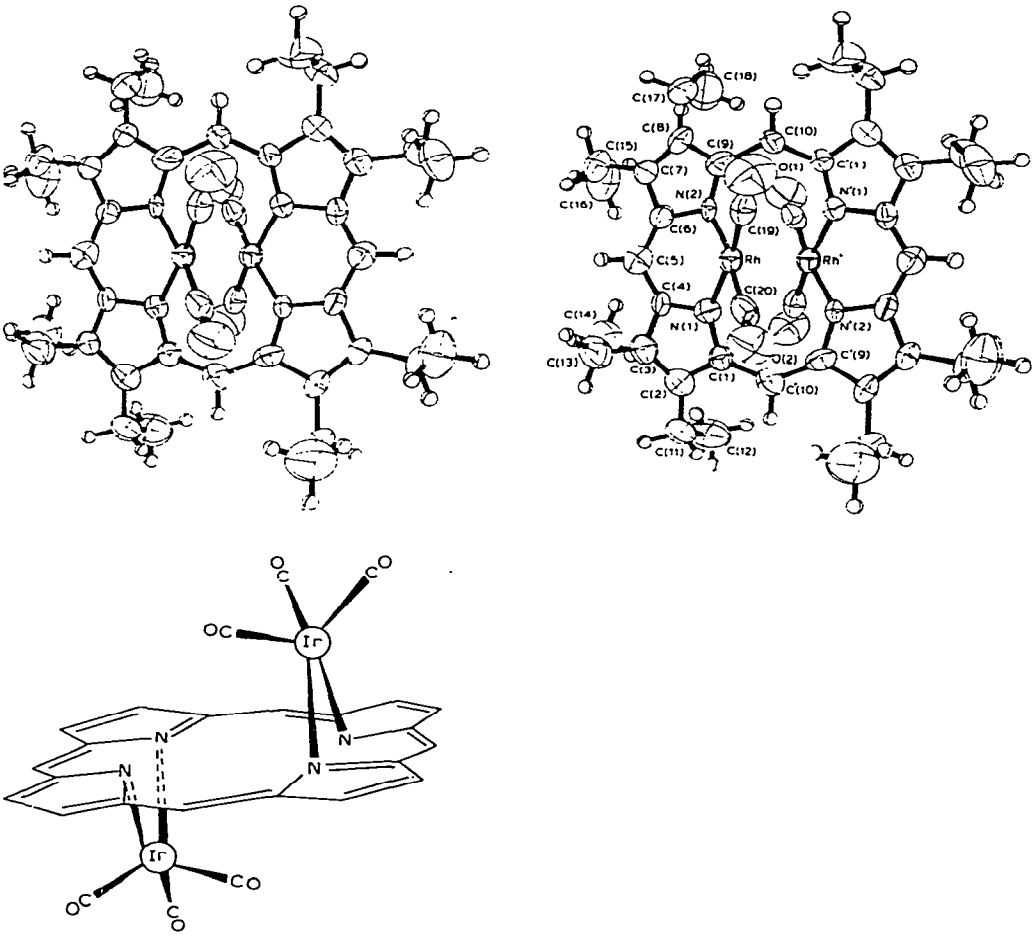

Fig. 7. Computer drawing of the molecule of $[Rh(CO)_2]_2(OEP)$ from ref. 44, and proposed structure for $[Ir(CO)_3]_2(OEP)$.

TABLE 4
Examples of porphyrin thiocarbonyl complexes

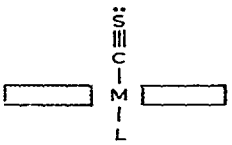

M	P	L	Ref.
Fe	TPP		36
Fe	TPP	Py	36
Fe	OEP		37
Fe	OEP	Py	37
Ru	OEP	Py	38
Os	OEP	Py	37

technetium mentioned above, the bonding between the porphyrin and the metal–carbonyl fragment may be slightly different. An X-ray structure determination of the bimetallic rhodium complex, $[Rh(CO)_2]_2(OEP)$ [44], again indicates a configuration in which one $Rh(CO)_2^+$ fragment is above and the other below the porphyrin plane (see Fig. 7). The coordination geometry of each Rh^I ion is now square planar with the ligand field consisting of two carbonyl molecules and two of the porphyrin nitrogens. A similarity in the spectroscopic properties of the rhodium and iridium complexes, $[Rh(CO)_2]_2(OEP)$ and $[Ir(CO)_3]_2(OEP)$ suggests that the iridium ion is also coordinated by two porphyrin nitrogens [28] but the greater π-basicity of Ir^I relative to Rh^I allows the coordination of three instead of two carbonyl groups. Figure 7 shows the X-ray structure of the rhodium complex and a schematic representation of the iridium complex.

(ii) Thiocarbonyl complexes

Due to the instability of the thiocarbonyl ligand under ambient conditions [45], relatively few complexes containing this ligand are known. Until recently, this ligand had never been incorporated into a porphyrin complex. Iron, ruthenium and osmium porphyrins containing the thiocarbonyl ligand have now been synthesized and are represented in Table 4. The synthetic methods employed utilize the reduction of thiophosgene, $CSCl_2$, or the desulfurization of coordinated CS_2 to generate the CS ligand in situ.

All of the porphyrin thiocarbonyls form hexacoordinate complexes of the type M(P)CS(L), where M = Fe, Ru, Os; P = TPP (for Fe) and OEP; and

L = amine. Only in the case of iron is the equilibrium constant for the reaction

$$Fe(P)CS + L \overset{K}{\rightleftharpoons} Fe(P)CS(L) \quad (3)$$

small enough to allow the isolation of the pentacoordinate complex [36,38].

A comparison of the spectroscopic properties [38] of the isostructural series M(OEP)CO(Py) and M(OEP)CS(Py), where M = Fe, Ru and Os, confirms the previous assertion that CS is a stronger π-acceptor ligand than CO [46,47]. Greater metal–CS bond strength is also indicated by the increased stability of the Fe(P)CS(L) complexes toward autoxidation relative to Fe(P)CO(L).

(iii) Carbene complexes

The carbene fragment, CX_2, has long been postulated as an intermediate in organic reactions [48] but was first shown to be a ligand for transition metal complexes in 1964 [49]. The observation that a variety of organic halides react with ferrous cytochrome P450 to give stable complexes [50] led to the postulate of iron–carbene intermediates in these biological systems. Further investigation of synthetic ferrous porphyrins as model compounds revealed a general synthetic method [39–41] for preparing the remarkably stable iron–carbene complexes represented by the equation

$$Fe^{II}(P) + CX_4 + 2\,e^- \rightarrow Fe(P)CX_2 + 2\,X^- \quad (4)$$

As is the case with the pentacoordinate carbonyl and thiocarbonyl complexes, the pentacoordinate carbene complexes of ferrous porphyrins show a large affinity for a second axial ligand.

$$Fe(P)CX_2 + L \overset{K}{\rightleftharpoons} Fe(P)CX_2(L) \quad (5)$$

The magnitude of K is markedly dependent on the nature of the carbene substituents X as well as the ligand field strength of L [40]. However, coordination of a sixth ligand destablizes the iron–carbene bond and significantly enhances the rate of autoxidation [40].

Table 5 lists some of the compounds prepared according to eqn. (4). The crystal structure of the dichlorocarbene complex, $Fe(TPP)CCl_2(H_2O)$ [41] is shown in Fig. 8, confirming the carbenic nature of the axial ligand. Of particular interest are the carbene complexes shown in Fig. 9, derivatives of the insecticide DDT [42] and the insecticide synergist of the 1,3-benzodioxole series [43]. The biological implications of these compounds in chemistry of the cytochrome P450 enzyme system will be discussed in a subsequent section.

TABLE 5
Examples of porphyrin carbene complexes

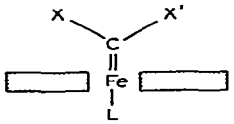

P	X	X′	L	Ref.
TPP	Cl	Cl		39
TPP	Cl	Cl	EtOH	40
TPP	Cl	Cl	Py	40
TPP	Cl	Cl	*N*Me-Im	40
TPP	F	Cl		40
TPP	F	Br		40
TPP	Br	Br		40
Proto IX	Cl	Cl		41

The reaction between ferrous porphyrins and carbon tetraiodide according to eqn. (4), results in the formation of the μ-bridged carbido complex (see Section F) $[Fe(TPP)]_2C$ [40]. This reaction presumably proceeds via the diiodocarbene intermediate, $Fe(TPP)CI_2$.

(iv) Metal–carbon σ-bonded complexes

The first example of organometallic bonding in biochemical systems was provided by the vitamin B_{12} coenzyme [50,51]. The biochemically active form of the coenzyme is a corrinoid complex of Co(III) with a covalent bond between the cobalt ion and the 5′-carbon of an adenine moiety. Porphyrin complexes of Co(III) have also been shown capable of forming metal–carbon sigma bonds with several different organic ligands [52]. Examples of these and other metalloporphyrins with metal–carbon sigma bonds are listed in Table 6.

The coordination geometry of these complexes is either square pyrimidal or pseudo-octahedral. A variety of organic residues have been reported as ligands such as alkyl, aryl, acyl, σ-allyl and alkoxycarbonyl. Some of the more common synthetic methods include:

(a) Reaction of a porphyrin metal halide with the appropriate Grignard reagent

$$M(P)X + RMgX \rightarrow M(P)R + MgX_2 \quad (6)$$

(b) Reaction of the univalent metalloporphyrins with alkyl halides

$$[M^I(P)]^- + RX \rightarrow M(P)R + X^- \quad (7)$$

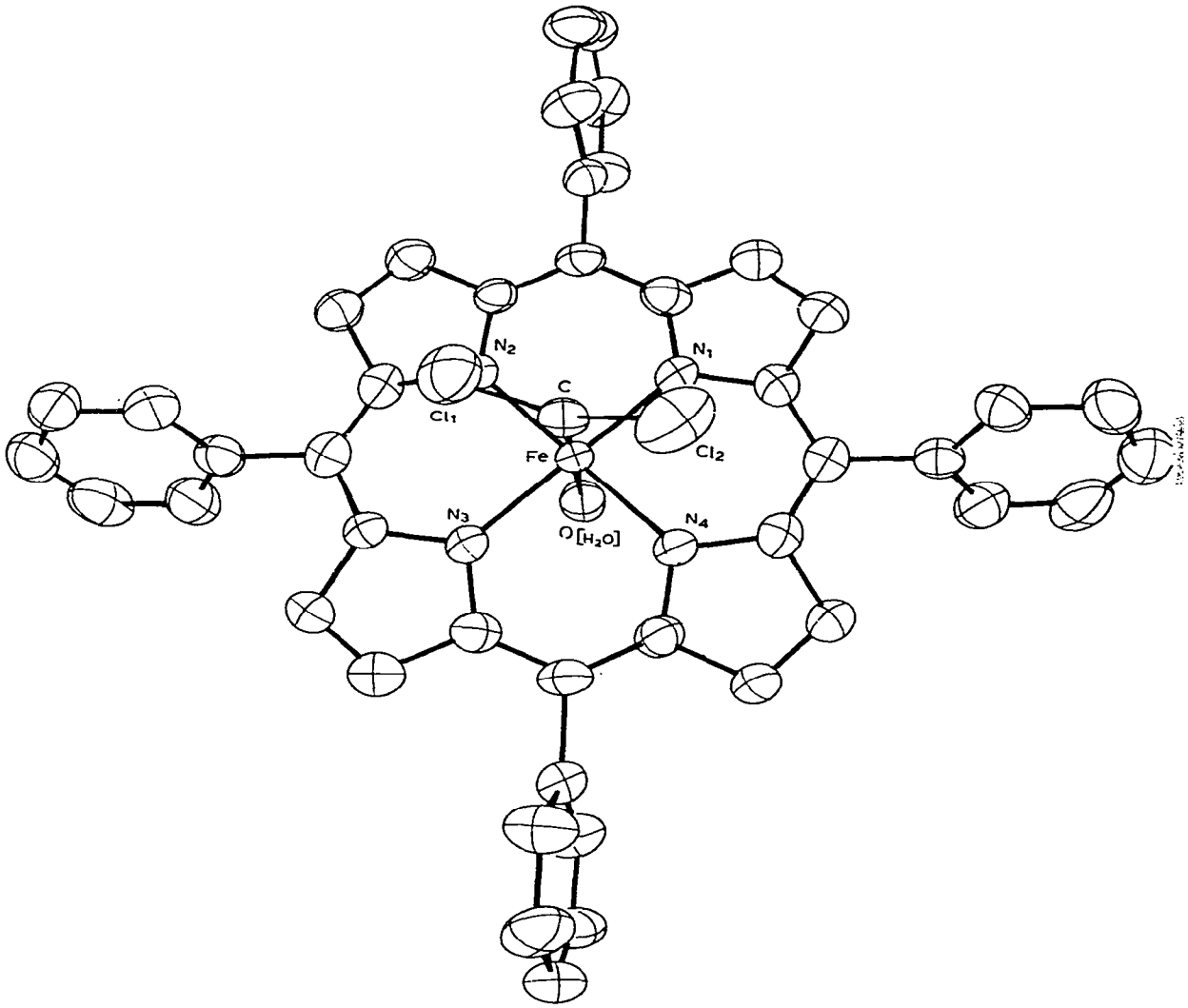

Fig. 8. Computer drawing of the molecule $Fe(TPP)CCl_2(H_2O)$ from ref. 41.

Fig. 9. Schematic representation of the carbene derivatives of (a) DDT and (b) 1,3-benzodioxole from refs. 42 and 43, respectively.

TABLE 6
Examples of metal–carbon σ-bonds in metalloporphyrin ligand systems

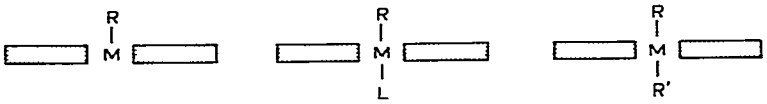

M	P	R	L	R′	Ref.
Co	Etio-I	Me	H_2O		52
Co	Etio-I	Ph	H_2O		52
Co	Etio-I	$COCH_3$	H_2O		52
Co	Etio-I	CH_2CH_2OH	H_2O		52
Fe	Etio-I	*p*-Tol	H_2O		52
Fe	Etio-I	Et	H_2O		52
Co	TPP	CH_2Cl			55
Co	TPP	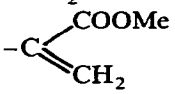			55
Rh	OEP	Me			60
Rh	TPP	$COCH_3$			61
Rh	TPP	COOEt			27
Ir	OEP	Me			28
Ir	OEP	C_8H_{13} [a]			28
Ge	TPP	Et		Et	62
Ge	TPP	CH_2SiMe_3		CH_2SiMe_3	62
Sn	TPP	Et		Et	62
Sn	TPP	CH_2SiMe_3		CH_2SiMe_3	62

[a] Cyclooctenyl.

Metal–carbon σ bonds are formed also, of course, by direct addition of isocyanides [53].

A number of more novel reactions have led to formation of metal–carbon bonds. The dicarbonylrhodium(I) complex $[Rh(CO)_2]_2$(Etio-I) undergoes oxidative addition reactions with a variety of substrates to form organometallic Rh(III) complexes [54] according to the reaction

$$[Rh(CO)_2]_2(\text{Etio-I}) + RX \rightarrow Rh(P)R + Rh(CO)_2^+ + X^- \quad (8)$$

Cobalt(III) porphyrins react with diazoalkanes to give vinyl- or halomethyl-complexes [55].

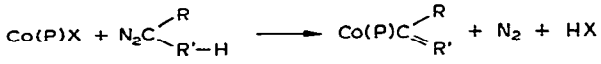

(9)

As mentioned in Section C(i), nucleophilic attack by ethoxide ion on the weakly coordinated carbonyl ligand in Rh(TPP)CO(Cl) leads to an ethoxy-

carbonyl complex [27]

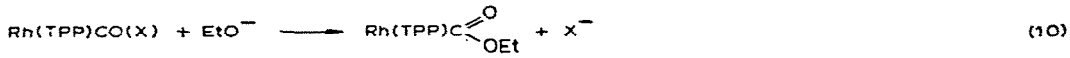

(10)

The chlororhodium(III) complex, $Rh(OEP)Cl(H_2O)$, reacts with ethyl vinyl ether [56] according to the reaction

$$Rh(OEP)Cl(H_2O) + CH_2 = CH-OEt \xrightarrow{EtOH} Rh(OEP)-CH_2CH(OEt)_2 \quad (11)$$

The 2,2-diethoxyethyl ligand hydrolyzes to give the formylmethyl rhodium complex

$$Rh(OEP)-CH_2CH(OEt)_2 \xrightarrow{H^+} Rh(OEP)-CH_2CHO \quad (12)$$

$Rh(OEP)Cl(H_2O)$ also reacts with acetylenes [56] to give a variety of products

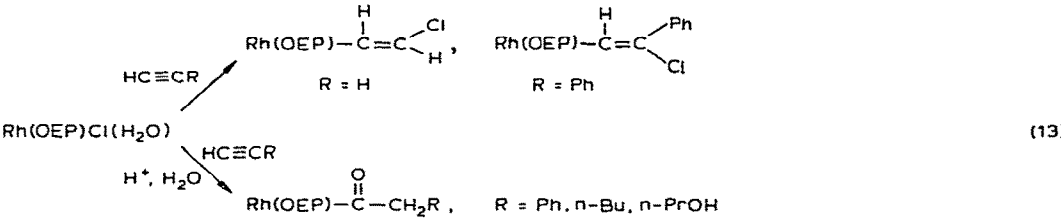

(13)

An interesting feature of cobalt–alkyl porphyrins is the migration of the alkyl group from the metal to a porphyrin nitrogen upon oxidation of the porphyrin macrocycle. The migration is reversible since reduction back to the neutral complex yields the original metal–alkyl complex [57].

(14)

A similar methyl migration is also observed in *N*-methyl dirhodium(I) porphyrins [58]. This type of migration may also be related to the appearance of *N*-alkylated protoporphyrins as the so-called "green pigments" of several hemoprotein systems [59].

D. METAL–NITROGEN BONDING

(i) Dinitrogen complexes

The first transition metal complex to incorporate the nitrogen molecule as a ligand, $[Ru(NH_3)_5N_2]Cl_2$, was synthesized by Allen and Senoff [63] in 1965. Since then, many dinitrogen complexes have appeared in the literature

TABLE 7
Examples of porphyrin dinitrogen complexes

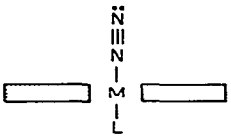

M	P	L	Ref.
Fe	Proto IX-DME	Py	65
Ru	OEP	THF	66
Os	OEP	THF	67
Os	TPP	THF	68

[64], and the field has taken on special interest with respect to the problem of biological nitrogen fixation.

Table 7 lists the dinitrogen complexes of metalloporphyrins. Although the iron [65] and ruthenium [66] derivatives have been reported, only the dinitrogen complexes of osmium porphyrins [67,68] are stable enough to allow extensive characterization. The osmium complexes are pseudo-octahedral and are isostructural with the corresponding carbonyl derivatives. The IR spectrum shows the characteristic $\nu(N \equiv N)$ at 2110 and 2032 cm^{-1} for $Ru(OEP)N_2(THF)$ and $Os(OEP)N_2(THF)$, respectively. Attempts to

TABLE 8
Examples of porphyrin nitrosyl complexes

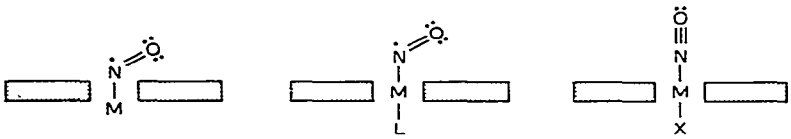

M	P	L	X	Ref.
Mn	TPP			69
Mn	TPP	4Me-Pip		69
Fe	TPP			70
Fe	TPP	*N*Me-Im		73
Co	TPP			71
Mo	TTP	MeOH [a]		26
Ru	OEP		OMe	11
Os	OEP		OMe	74

[a] *Cis* configuration of NO and MeOH ligands.

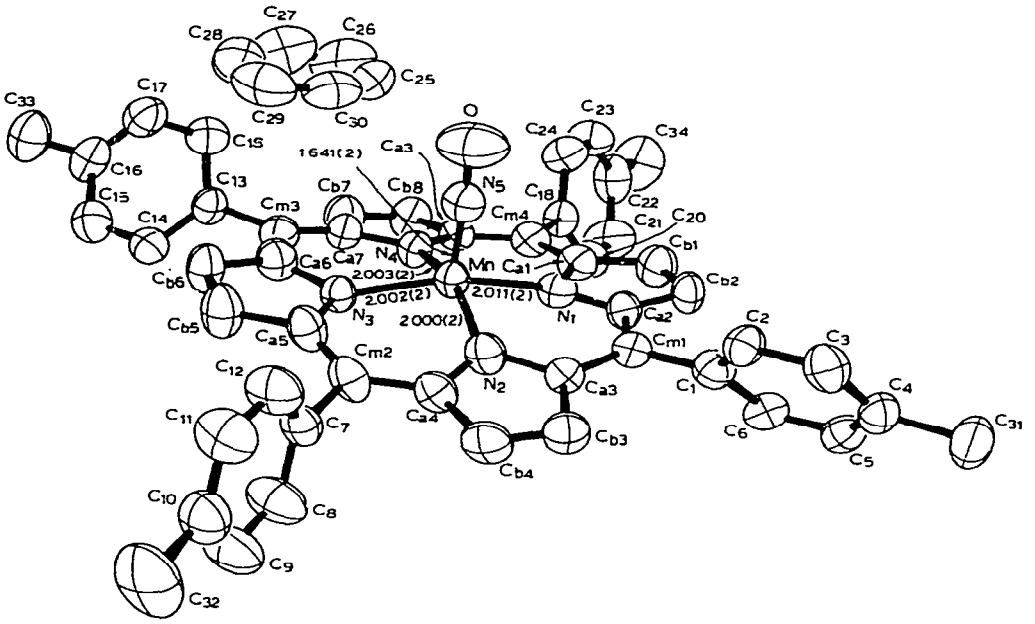
C27
C28
C26
C25
C29
C30
C33
C17
C23
O
C24
C34
1641(2)
Ca3
C15
C16
N5
C13
Cb7
Cb8
C18
C22
C15
Cm3
Cm4
C21
C20
C14
Cb1
Ca6
Ca7
N4
Mn
Ca1
2.003(2)
Cb6
Cb2
2.002(2)
2.011(2)
N3
2.000(2)
N1
Ca2
C2
Cb5
Ca5
Cm2
Cm1
C3
N2
Ca3
C1
C12
C4
C11
C7
Ca4
Cb3
C6
C31
Cb4
C5
C10
C8
C9
C32

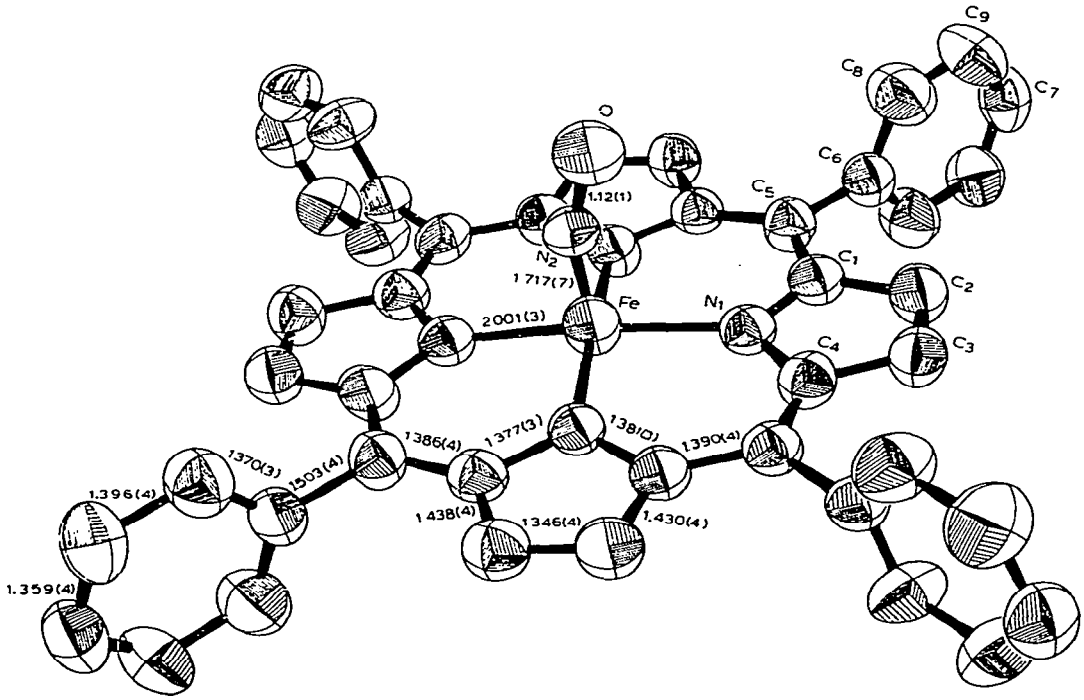
C9
C8
C7
O
C6
1.12(1)
C5
N2
C1
1.717(7)
C2
Fe
N1
2.001(3)
C4
C3
1.386(4)
1.377(3)
1.381(1)
1.390(4)
1.370(3)
1.503(4)
1.396(4)
1.438(4)
1.346(4)
1.430(4)
1.359(4)

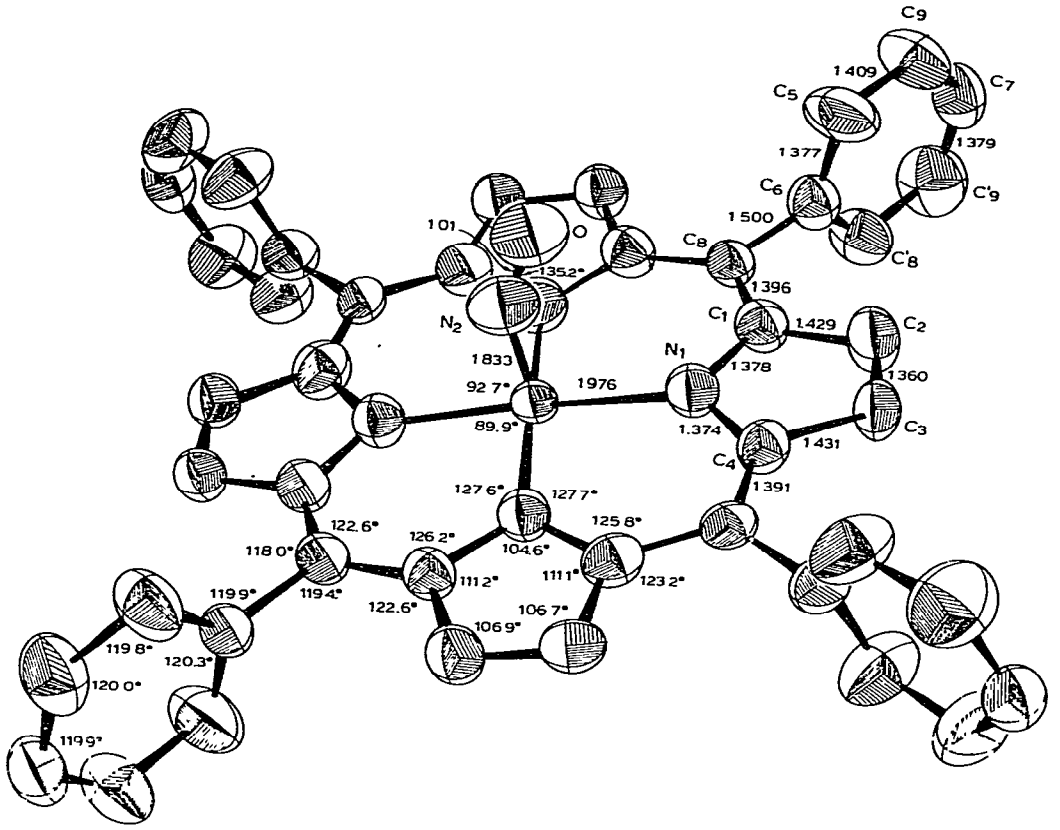

Fig. 10. Computer drawing of the molecules (a) Mn(TPP)NO, (b) Fe(TPP)NO and (c) Co(TPP)NO from refs. 69–71, respectively.

substitute the THF ligand with a stronger field ligand such as Py or *N*Me-Im leads to displacement of the dinitrogen ligand and formation of the bis complexes $Os(OEP)L_2$ [25,68].

(ii) Nitrosyl complexes

Several examples of mononitrosyl derivatives of metalloporphyrins are listed in Table 8.

Most of these complexes have either square pyramidal or pseudo-octahedral coordination geometries. The X-ray crystal structures of the five-coordinate complexes Mn(TTP)NO [69], Fe(TPP)NO [70] and Co(TPP)NO [71] are shown in Fig. 10. The basic structural features are illustrated schematically in Fig. 11. Several trends are noticeable in a comparison of these structures:

(a) The M–N–O bond angles decrease along the series Mn (ca. 180°) > Fe (ca. 150°) > Co (ca. 130°).

(b) The metal–nitrogen (NO) distances increase in the order Mn (1.641 Å) < Fe (1.717 Å) < Co (1.833 Å).

(c) The displacement of the metal from the mean plane of the four porphyrin nitrogen decreases along the same series Mn (0.34 Å) > Fe (0.21 Å) > Co (0.09 Å).

These observations may be rationalized in terms of π-bonding and non-bonding repulsions between the axial ligand (NO) and the porphyrin core [69]. The $[MNO]^6$ electronic configuration [72] of the Mn complex favors the linear NO geometry thus maximizing π-backbonding. This manifests itself in shorter $M-N_{NO}$ bond distances. The relatively large displacement of the Mn ion from the mean porphyrin plane minimizes the non-bonding repulsions between the nitrogens of the nitrosyl ligand and porphyrin core which arise from the short $M-N_{NO}$ bond distances. In the $[MNO]^7$ and $[MNO]^8$ configurations of the respective iron and cobalt complexes, the expected [72] bending of the nitrosyl ligand is observed to provide a low energy non-bonding orbital on the nitrosyl nitrogen for the additional *d* electrons of the metal, thus lowering the total energy of the complex. The bending of the nitrosyl ligand disrupts the metal–ligand π-bonding and results in longer $M-N_{NO}$ bond distances. As the length of the $M-N_{NO}$ bond increases, the nitrogen–nitrogen repulsions decrease, thus allowing the low spin metal ion

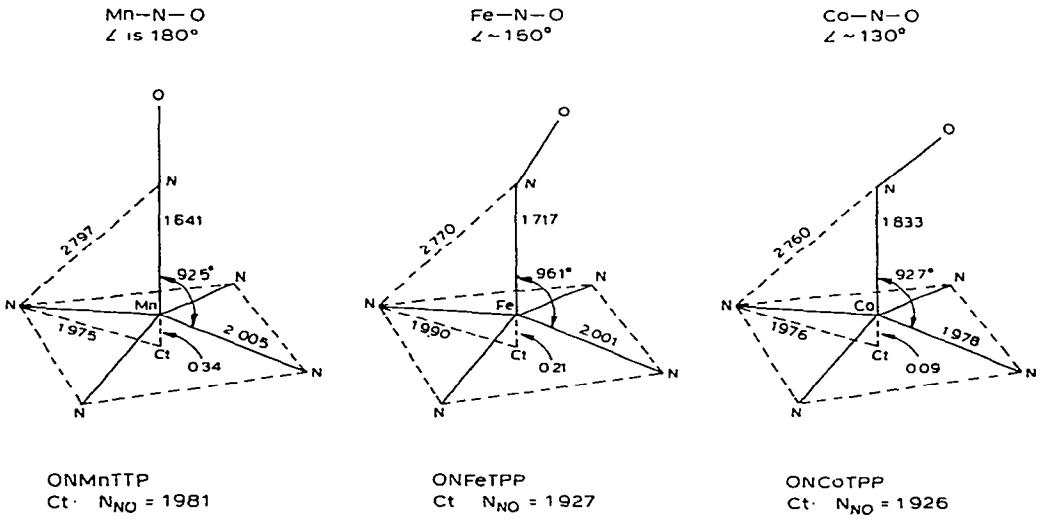

Fig. 11. Comparison of the coordination geometries of the pentacoordinate nitrosyl complexes Mn(TPP)NO, Fe(TPP)NO and Co(TPP)NO from ref. 69.

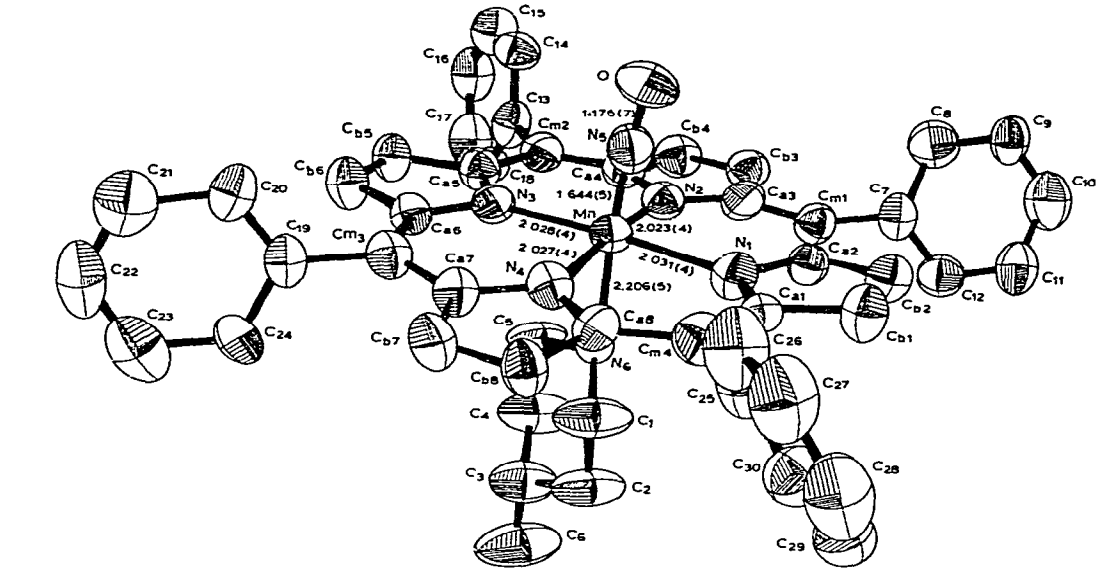

a

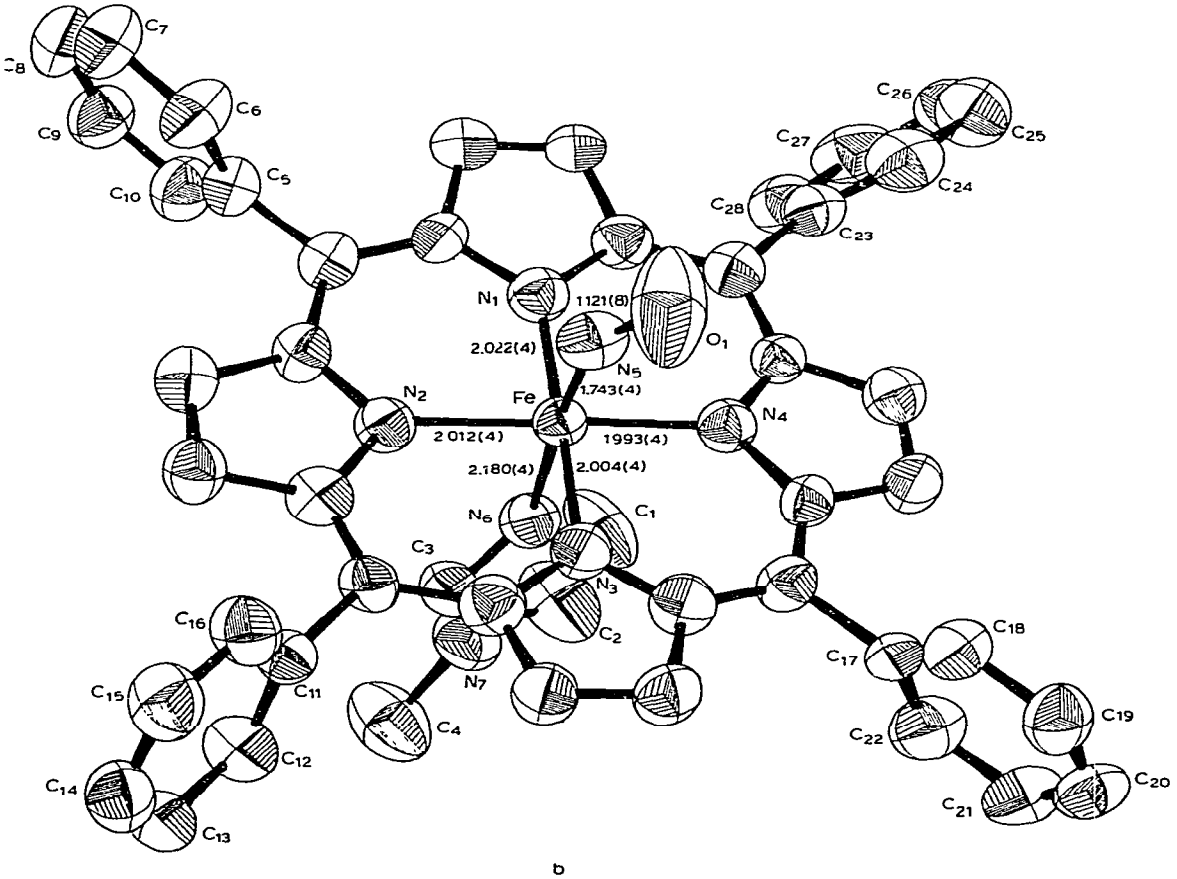

b

Fig. 12. Computer drawing of the molecules (a) Mn(TPP)NO(4Me-Pip) and (b) Fe(TPP)NO(*N*Me-Im) from refs. 69 and 73, respectively.

to assume a more planar arrangement with respect to the porphyrin core.

The X-ray crystal structures of the six coordinate complexes Mn(TPP)-NO(4Me-Pip) [69] and Fe(TPP)NO(*N*Me-Im) [73] are presented in Fig. 12. The significant structural changes observed in going from the five- to the six-coordinate Mn and Fe complexes may be summarized as follows:

(1) Virtually no difference is observed in the $M-N_{NO}$ bond lengths of the Mn derivatives, and only a slight increase, 1.72 to 1.74 Å, was observed upon coordination of the *N*Me-Im ligand in the iron complex.

(2) The M–N–O bond angle appears to decrease slightly when a strong

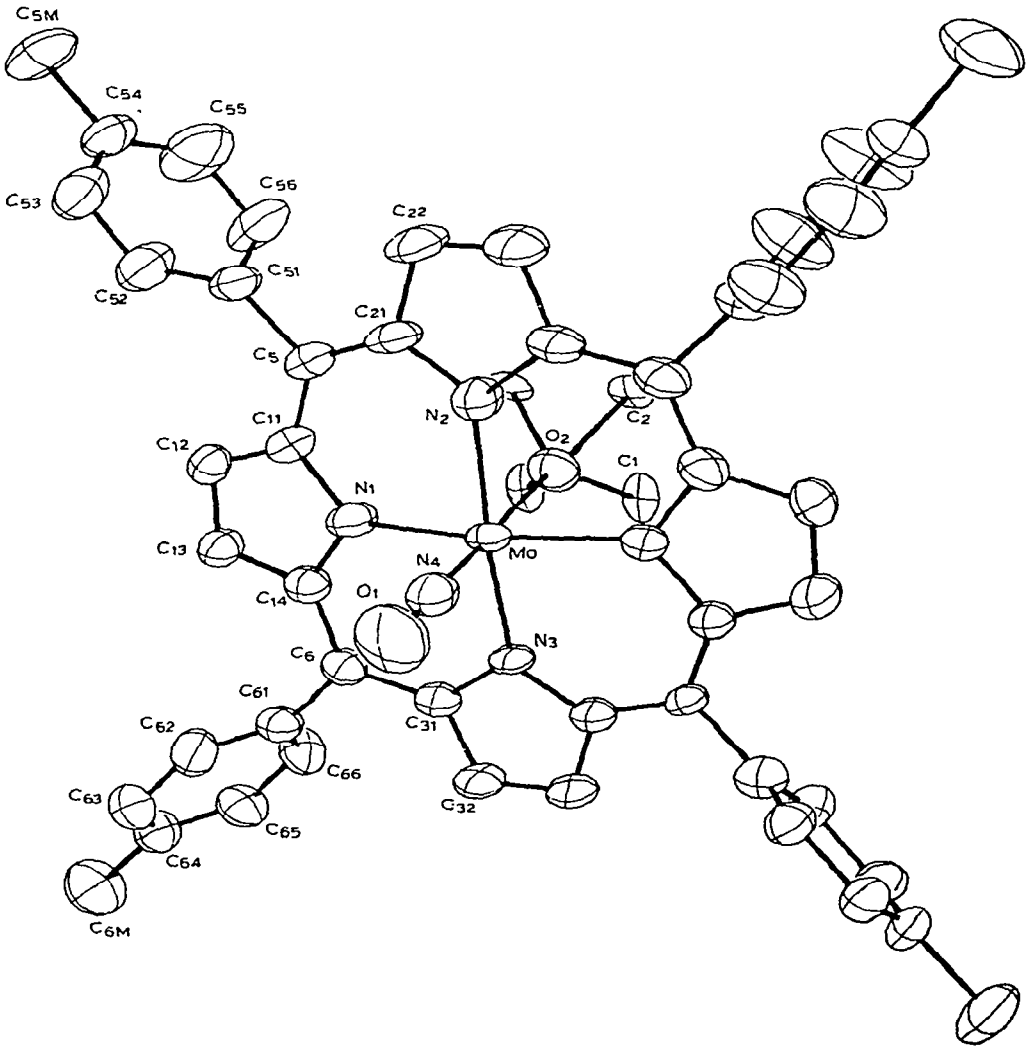

Fig. 13. Computer drawing of the molecule Mo(TPP)NO(MeOH) from ref. 26.

field ligand coordinates *trans* to the nitrosyl ligand; for the Fe derivatives, the change in the M–N–O angle is about 10°.

(3) A remarkable change is observed in the displacement of the metal atom from the mean plane of the porphyrin nitrogens. In the Mn complexes, the metal ion moves from 0.34 Å out of the plane to 0.10 Å upon coordination of the 4Me-Pip ligand and in the Fe complexes from 0.21 to 0.07 Å upon coordination of the *N*Me-Im ligand.

The X-ray crystal structure of the hexacoordinate Mo(TPP)(NO)(MeOH) complex [26] is shown in Fig. 13. Notable features are a linear NO ligand with ⟨Mo–N–O = 179.8° and a 0.28 Å displacement of the Mo ion from the mean plane of the porphyrin core.

The isostructural ruthenium and osmium mononitrosyl derivatives, Ru(OEP)NO(OMe) [11] and Os(OEP)NO(OMe) [74] are both diamagnetic with the $[MNO]^6$ configuration. The IR stretching frequencies of $\nu(NO) = 1780$ and 1745 cm^{-1} (Ru and Os, respectively) are characteristic of a linear NO^+ ligand.

The only well characterized dinitrosyl metalloporphyrins are $Mo(TPP)(NO)_2$ [26] and $Os(OEP)(NO)_2$ [74]. The former has the *cis* configuration of nitrosyl ligands whereas the latter has the *trans* configuration as represented in Fig. 14. The crystal structure of $Mo(TPP)(NO)_2$ is shown in Fig. 15. In addition to the *cis* configuration of nitrosyl ligands the note-

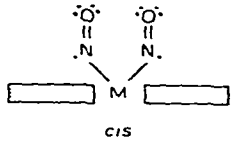

cis

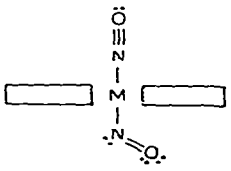

trans

Fig. 14. Schematic representation of the *cis* and *trans* geometries for the dinitrosyl complexes, $Mo(TPP)(NO)_2$ and $Os(OEP)(NO)_2$, respectively.

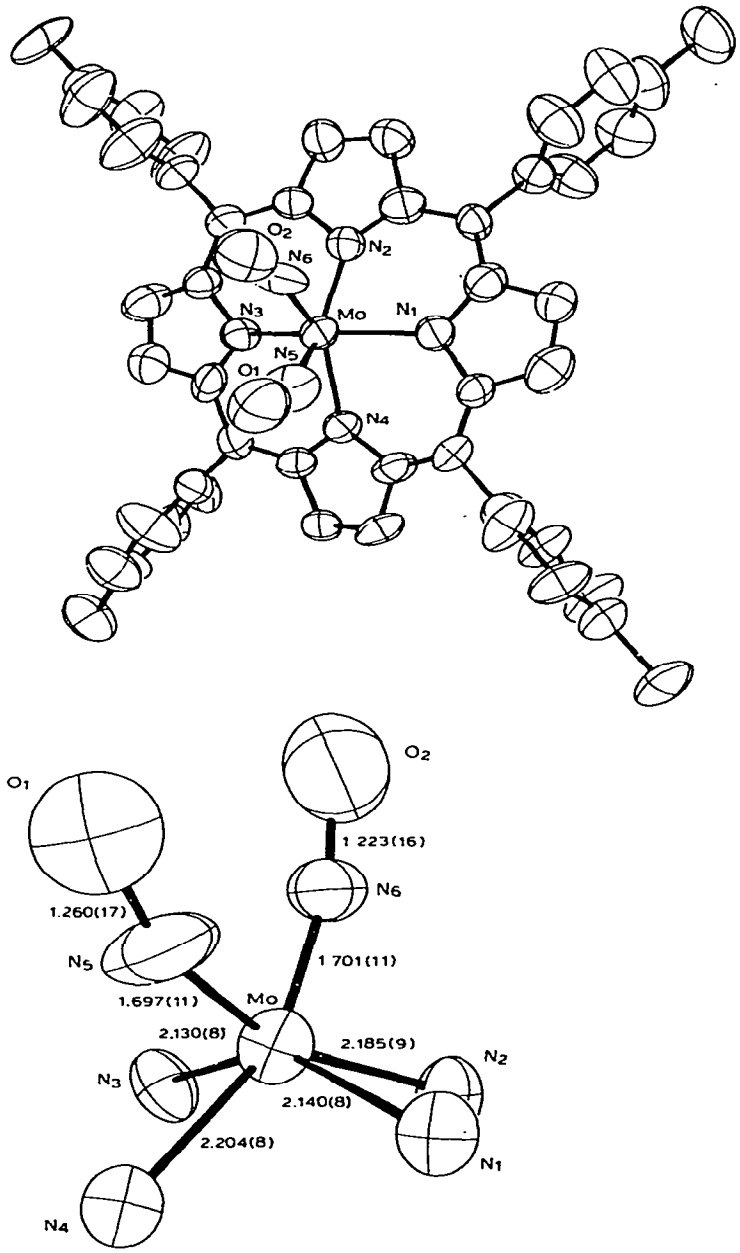

Fig. 15. Computer drawing and inner coordination sphere of the molecule $Mo(TPP)(NO)_2$ from ref. 26.

worthy features of this structure are: (a) a displacement of 0.99 Å of the Mo ion from the mean porphyrin plane toward the nitrosyl ligands; (b) an averaged Mo–N–O bond angle of 158°; and (c) a bending of the nitrosyl

TABLE 9
Examples of porphyrin nitrido complexes

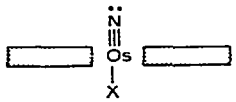

P	X	Ref.
OEP	OMe^-	25,76
OEP	F^-	25,76
OEP	$OClO_3^-$	25,76

groups toward each other. No crystal structure is available for the osmium derivative but IR stretching frequencies of $\nu(NO) = 1779$ and 1500 cm^{-1} are indicative of one linear (NO^+) and one bent (NO^-) nitrosyl ligand.

(iii) Nitrido complexes

With the exception of the μ-bridged iron nitrido complex $[Fe(TPP)]_2N$ discussed in a subsequent section, the only examples [75] of the coordinated nitride ligand, N^{3-}, in metalloporphyrin chemistry come from the systems Os(OEP)N(X) [25,76]. Table 9 illustrates several complexes of the osmium–nitrido system. The nitride ligand is obtained from the oxidation of coordinated ammonia by peracetic acid in protic solvent

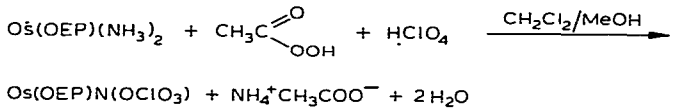

$$Os(OEP)(NH_3)_2 + CH_3C(=O)OOH + HClO_4 \xrightarrow{CH_2Cl_2/MeOH} Os(OEP)N(OClO_3) + NH_4^+CH_3COO^- + 2H_2O \quad (15)$$

or by autoxidation in an aprotic solvent

$$2\ Os(OEP)(NH_3)_2 + 2\ O_2 \xrightarrow{C_6H_6} \text{“}[Os(OEP)N]_2O\text{”} + 2\ NH_3 + 3\ H_2O$$

$$\text{“}[Os(OEP)N]_2O\text{”} + 2\ MeOH \rightarrow 2\ Os(OEP)N(OMe) + H_2O \quad (16)$$

The latter reaction most likely involves the μ-oxo linked nitrido species, $[Os(OEP)N]_2O$, which readily undergoes methanolysis to yield the methoxide derivative Os(OEP)N(OMe). The strong *trans* influence of the nitride ligand in this complex is evident from the low Os–O stretching frequency $\nu(Os–O) = 410$ cm^{-1}. This in turn facilitates the displacement of the methoxide ligand by the conjugate base of a strong acid

$$Os(OEP)N(OMe) + HF \rightarrow Os(OEP)N(F) \quad (17)$$

$$Os(OEP)N(OMe) + HClO_4 \rightarrow Os(OEP)N(OClO_3) \quad (18)$$

The coordinated mode of the perchlorate ligand is verified by the splitting of the IR band at 620 cm^{-1} [77,78].

E. METAL–OXYGEN BONDING

The interaction of dioxygen with metalloporphyrins remains a topic of extreme interest. Synthetic O_2-carriers generally have been known for some forty years and such species have always had scientific appeal because of the role of such centers in naturally occurring oxygen-storage and -transport systems; for example, myoglobin and hemoglobin, respectively. Nature evolved several prosthetic groups for such functions as well as for activating O_2 via enzymic oxygenases, which incorporate one or two atoms of O_2 to a substrate, or via oxidases that convert both atoms of O_2 to water or hydrogen peroxide. One particularly prevalent active site within such systems is an iron porphyrin moiety (the heme unit); it is the prosthetic group,

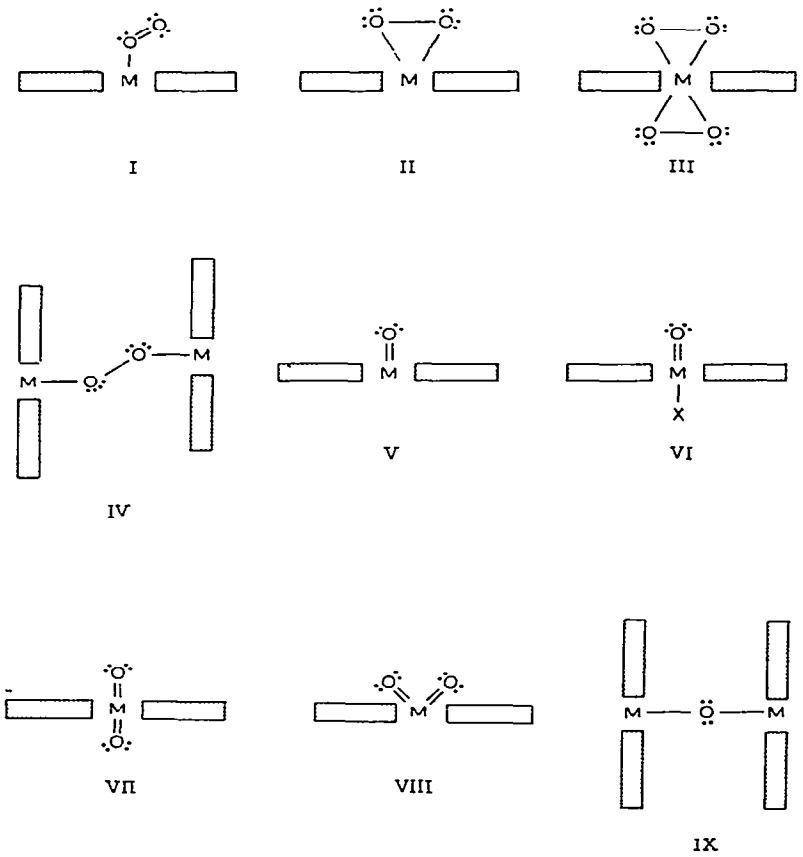

Fig. 16. Major types of metalloporphyrin oxygen complexes.

for example, in myoglobin, hemoglobin, P450 monooxygenase, tryptophan dioxygenase, and cytochrome c oxidase. The enzymes catalase and peroxidase, both containing heme centers, utilize hydrogen peroxide and are related to the dioxygen systems.

Studies on oxygen-containing metalloporphyrins outside of a protein environment are clearly important for an increased understanding of the structure and function of biological systems utilizing oxygen, and for the development of catalysts that mimic the enzymes.

The subject has been very extensively reviewed in recent years [79–95] and access to the vast literature on metalloporphyrin-O_2 interactions both in the presence and absence of proteins can be made via these representative references. This section of the review will summarize the structural types of metalloporphyrin–oxygen species that have been found or postulated, and will also include recent advances in the area.

The structures shown in Fig. 16 represent the major types of protein-free metalloporphyrin–oxygen complexes that have been reported to date. The bridging μ-oxo structures (16-IX) will be considered in the following section.

The nature of the metal–oxygen bond has been studied using appropriate techniques that include especially: (1) the IR of the coordinated oxygen; (2) UV/VIS spectra (especially at subzero temperatures); (3) magnetic susceptibility measurements; (4) resonance Raman spectra; (5) ESR spectra; (6) Mossbauer spectra; and (7) the chemistry of the coordinated oxygen. X-ray crystallography has established the end-on geometry (16-I) for oxygenated iron(II) complexes of "picket-fence" porphyrins [96], as well as for oxymyoglobin [96,97] and oxycobaltmyoglobin [98].

(i) Coordinated dioxygen: superoxide and peroxide structures

Generally, attempts to form $L_nM(P)O_2$ species via reaction of O_2 with $L_nM(P)$ species (L = axial ligand) in solution at ambient temperatures result in formation of bridged oxo species (16-IX), or bridged peroxo species (16-IV). One mechanism for the oxidation [87,99,100] is outlined in eqn. (19)

$$M^{II} + O_2 \overset{K_{O_2}}{\rightleftharpoons} M^{II}(O_2) \xrightarrow[M^{II}]{k} M^{III}-O_2-M^{III} \quad \Big| \text{ several steps} \quad \rightarrow \quad M^{III}-O-M^{III} \tag{19}$$

but other mechanisms involving noncoordinated O_2 (outer sphere processes) are also possible [101–103]. Stabilization of the $M^{II}(O_2)$ species has been accomplished by decreasing the rate constant k which has been realized by: (1) the use of subzero temperatures [79,87,89,90]; (2) the design and synthe-

sis of picket-fence porphyrins [91,96] and various capped or bi-capped porphyrins [104–108]; (3) supporting the metalloporphyrin on both inorganic [109] and organic polymers [110] via the axial ligand or substituent on a pyrrole ring; and (4) using a metalloporphyrin in the solid state [96,111,112]. In enzyme systems (including myoglobin and hemoglobin, the "honorary enzymes") the protein plays the role of the polymer support. Mention should also be made of flash photolysis studies under CO/O_2 atmospheres that allow for direct kinetic studies on the $M^{II}(O_2)$ species [113].

Irreversible oxygenation of Cr(II) and reversible oxygenation of Fe(II) and Co(II) porphyrins can yield species of type 16-I; in each case there is an axial donor ligand, usually an amine, *trans* to the dioxygen. As a result of some electron transfer from the metal to the dioxygen, the latter is described as an end-on superoxide moiety, and 16-I is frequently designated as $M^{III}O_2^-$. The notation, although unconventional, clearly does not imply that the dioxygen is ionically bound superoxide or covalently bound with a charge of -1. The nature of the metal–dioxygen link and the difficulty of assigning formal oxidation steps for types 16-I and 16-II has been discussed at length [e.g. refs. 114,115] and will not be considered further in this article. Structure 16-I is considered here to be a superoxide $^1\eta$-type species; 16-II and 16-III side-on $^2\eta$-peroxide species; 16-IV a bridged peroxide species; 16-V–VIII various terminal oxo species and 16-IX the bridge μ-oxo species. With cobalt, 16-I appears correctly described as a paramagnetic low-spin Co(III)-superoxide [114]; with Fe and Cr, the descriptions as diamagnetic spin-coupled M(III)-superoxides are more equivocal [114].

The nature of the bound O_2 and the second methylimidazole in a Fe(capped porp)(1 Me-Im)$_2O_2$ species remain to be established [106]. The speculative structure shown in Fig. 17 has been presented for a dimeric complex formed by reversible 1 : 1 O_2 binding by solid four-coordinate hemes; the oxygen atoms are considered to interact weakly with the Fe atoms and the adjacent parallel porphyrin planes [116].

A titanium(III) dioxygen adduct, FTi(TPP)O_2, formed reversibly by

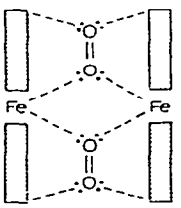

Fig. 17. Proposed structure for the reversible 1 : 1 O_2 binding by solid four-coordinate hemes.

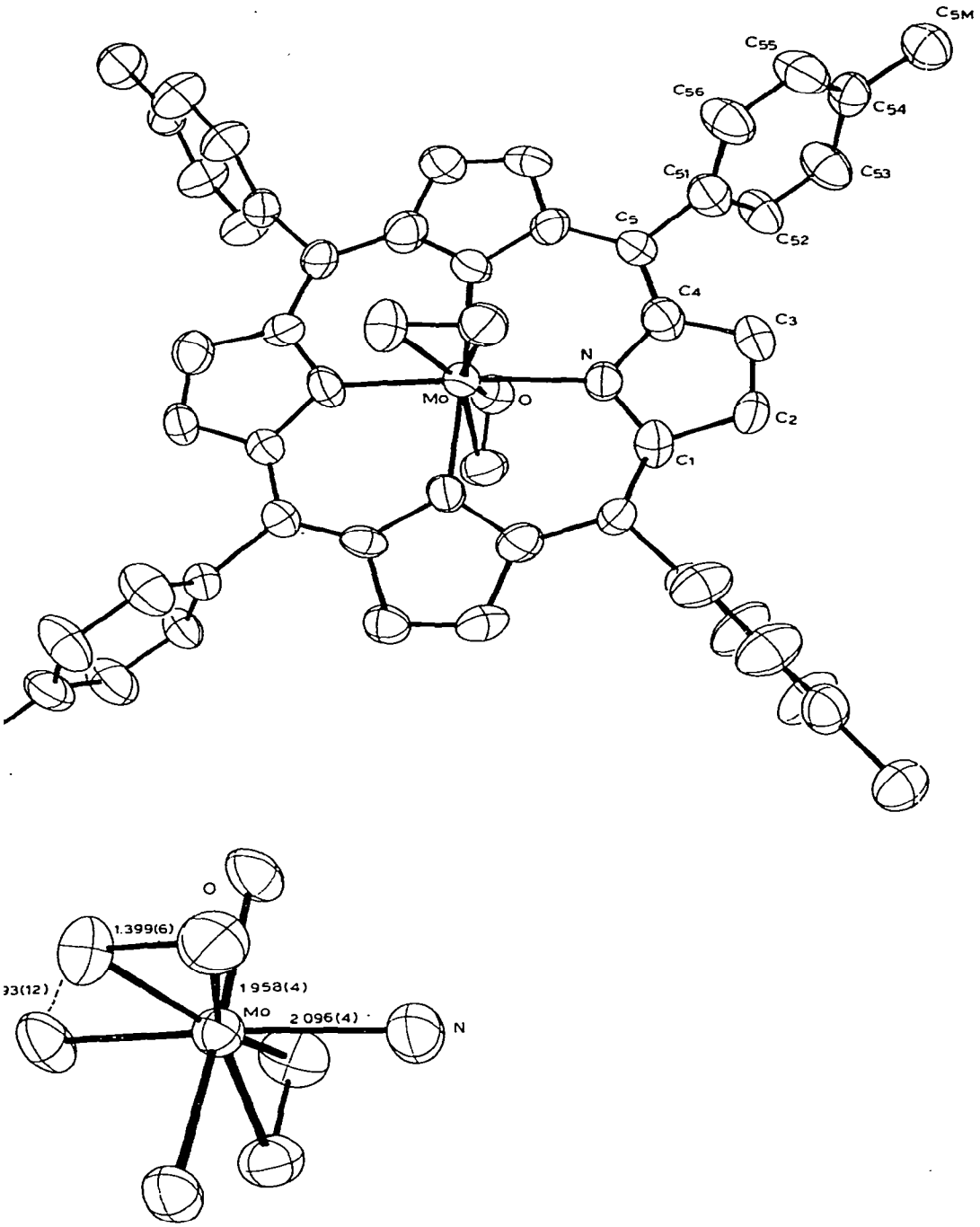

. 18. Computer drawing and inner coordination sphere of the molecule $Mo(TPP)(O_2)_2$ m ref. 121.

oxygenation of FTi(TPP) in host crystals of OTi(TPP), was considered initially to be a paramagnetic Ti(IV) superoxide [117,118], but a $Ti^{IV}(TPP^{+\cdot})$ peroxide formulation containing the porphyrin cation radical is now preferred in a seven-coordinate titanium center [119]. Without immobilization of the dioxygen adduct in the host lattice, the oxygenation yields a diamagnetic Ti(IV) peroxide of type 16-II with no *trans* axial ligand [117]. Such peroxides are more usually prepared by the reaction of H_2O_2 with the metal, in this case Ti(IV). This method has been used to isolate crystals of $Ti(OEP)O_2$, which has out-of-plane metal [120], and $Mo(TPP)(O_2)_2$ which has two orthogonal peroxide moieties (structure type 16-III), parallel to the porphyrin plane that also contains the metal [121]. The crystal structure of the latter is reproduced in Fig. 18.

Several Mn(II) dioxygen adducts synthesized via reaction (20)

$$Mn(P)Py + O_2 \rightleftharpoons Mn(P)O_2 + Py \qquad (20)$$

are formulated as type 16-II Mn(IV) peroxides [122,123], although some theoretical calculations [124] suggest other ground-state electronic configurations would be energetically more favorable. The isolation of a Mn(II) porphyrin with tetracyanoethylene with charge transfer to the olefin adds support to the Mn(IV) peroxide formulation [125].

Ruthenium(II) porphyrin complexes, the second row analogues of the biologically active Fe(II) species, have been found to bind O_2 reversibly at ambient conditions in certain polar aprotic solvents [66], although it remains unclear whether the 1 : 1 dioxygen adducts are of type 16-I or 16-II [66]. Reversible binding of ethylene [126], as well as SO_2 [126], by $Ru(OEP)(THF)_2$ suggests that a Ru(IV) peroxide 16-II is more likely [66]. There is no published report of any metal center that binds dioxygen as end-on superoxide 16-I, and C_2H_4 in the presumed familiar π-bonded mode, although solutions of (piperidine)Co(OMBP), that form the usual 1 : 1 type 16-I dioxygen complex at low temperature, have been found to react reversibly with C_2H_4 at ambient conditions [127].

A complex originally formulated Rh(II)(TPP) [128] has been reexamined and shown to be $Rh(TPP)O_2$ of type 16-I [129]. A very strong affinity for O_2 (removed only on heating to 150°C under high vacuum [129]) had misled the earlier workers, who had anticipated reactivity similar to that of cobalt(II) analogues [128].

Bridging peroxide, type 16-IV, species within metalloporphyrins have not been characterized by crystallographic techniques. However, they are almost certainly the final products of the O_2-oxidation of five-coordinate LCo(porp) complexes [130], this being based largely on cobalt(II) chemistry which has been well-established with Schiff base and other ligand systems [80,81,87]; regeneration of LCo(P) on heating the oxidation product under vacuum

supports the $[LCo(P)]_2O_2$ formulation more directly [131,132]. The lack of subsequent decomposition to a bridged oxo species (see eqn. (19)) has been rationalized on electronic grounds in that a suggested CoO intermediate (reaction (21)) requires an electron to be placed in a strongly antibonding π^* molecular orbital [133].

$$Co^{III}O_2Co^{III} \rightleftharpoons 2\ Co^{IV}O;\ Co^{IV}O + Co^{II} \rightarrow Co^{III}OCo^{III} \qquad (21)$$

Spectroscopic and other data at low temperatures give strong evidence for the existence of $Fe^{III}O_2Fe^{III}$, and for its decomposition via reaction (21), as well as via other processes [134,135]. An Fe(II) octaazamacrocyclic complex that binds 0.5 mole O_2 per Fe also appears to give a bridged peroxide [136]. Decomposition of the $Rh(TPP)O_2$ species in solution is also thought to give a bridged peroxide complex [129].

Bridging superoxide species, particularly well-documented for dinuclear cobalt(III) complexes with cyanide, ammonia or Schiff base ligands [80,81], have not been found within metalloporphyrin systems.

(ii) Oxo complexes

A wide range of oxo complexes of types 16-V and 16-VI are known. Some examples of the terminal oxo species are listed in Table 10. In the six-coordinate configuration M(P)O(X) there is a noticeable *trans* effect operating between the oxo ligand and the sixth ligand. The metal–oxygen stretching frequency $\nu(M=O)$ shows a marked dependence on the *trans* ligand X, the metal and the porphyrin substituents [25]. The niobium derivative Nb(TPP)O(AcO), shows a novel configuration in which the oxo ligand and

TABLE 10
Examples of porphyrin complexes with terminal oxo ligands

M	P	Ref.	M	P	X	Ref.
Ti	OEP	165,166	Re	OEP	F	158
Ti	Meso IX-DME	167	Re	OEP	OPh	170
V	OEP	165	Mo	OEP	F	158
V	Meso IX-DME	168	Mo	OEP	OMe	170
V	Etio-I	169	Mo	OEP	Cl	170
Mo	OEP	165	W	OEP	F	158
Mo	TPP	156	W	OEP	OMe	170
			W	OEP	Cl	170

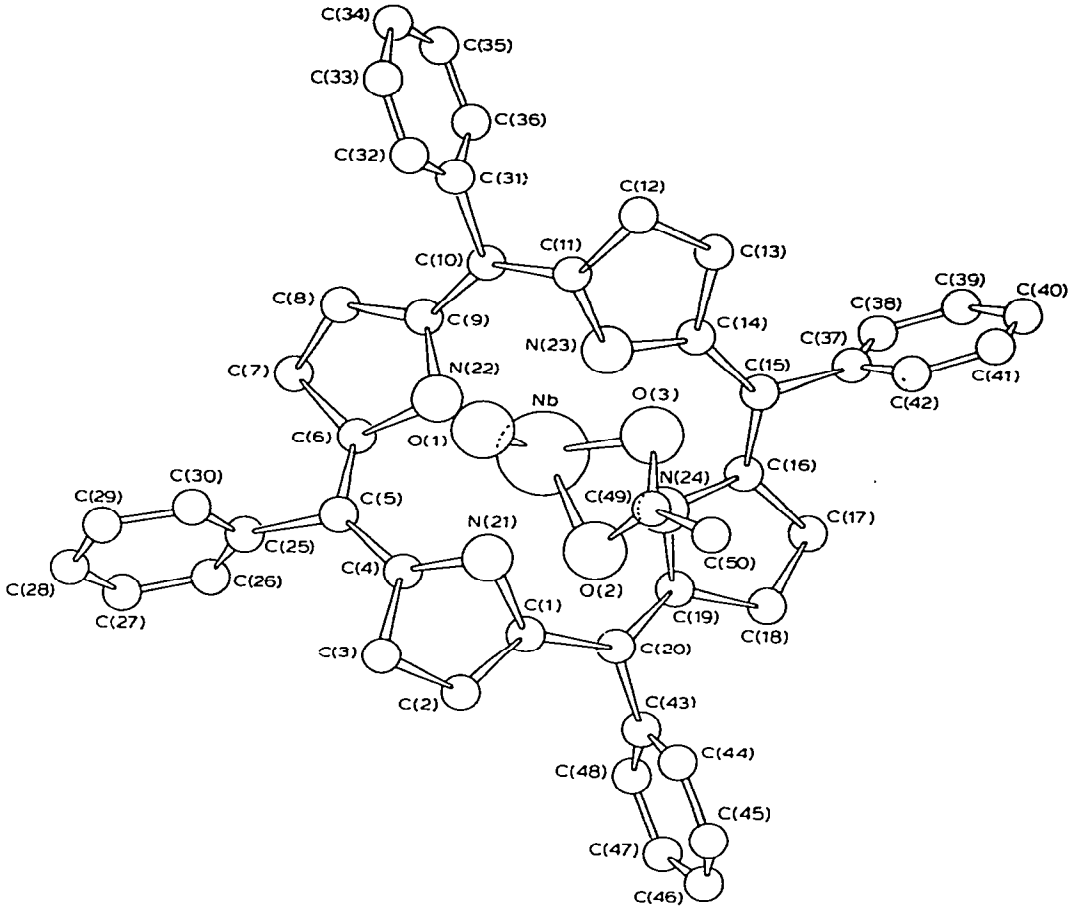

Fig. 19. Computer drawing of the molecule Nb(TPP)O(AcO) from ref. 137.

the bidentate acetate ligand are coordinated to the metal from the same side of the porphyrin, forming a tripod type, *cis* arrangement of axial ligands [137]. The crystal structure of this complex is shown in Fig. 19.

The *trans* dioxo structure 16-VII has been established for Os porphyrins made via H_2O_2 reactions [138], while a *cis* dioxo structure 16-VIII was found for $Mo(TPP)O_2$ formed via photolysis of the bisperoxo species [139]

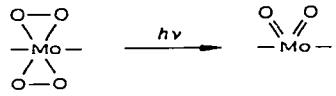

(22)

This *cis* dioxo complex stoichiometrically oxidizes phosphines, aldehydes and tetracyanoethylene via oxygen atom transfer [140], which may be relevant to the mechanism of O_2 activation by cytochrome P450 (see below).

(iii) Biological implications

There have been interesting developments in the inorganic chemistry of cytochrome P450, again in terms of the nature of the iron–dioxygen interaction and the mechanism of hydroxylation of a substrate RH according to reaction (23) [92,141,142]

$$RH + O_2 + 2\,e + 2\,H^+ \rightarrow ROH + H_2O \qquad (23)$$

The overall mechanism involves, (a) addition of RH to a low spin oxidized form (Fe^{III}) of the enzyme to give a high-spin enzyme–substrate complex; (b) addition of one electron to give a high-spin Fe^{II} system; (c) binding of O_2 to give a low spin dioxygen complex (analogous to oxymyoglobin except that the axial ligand *trans* to dioxygen is a cysteine thiolate [143]); (d) addition of the second electron to give what is formally an iron(I)–dioxygen system, and this intermediate breaks down to hydroxylated product, water, and the initial Fe(III) form of the enzyme. The only species not detected thus far in the enzyme system is the highly reactive Fe^IO_2 species. However, such protein-free iron porphyrin species have now been formed at low temperatures in

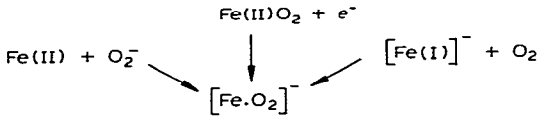

(24)

DMSO solutions via the three routes outlined in (24) [144–146] that is, by reaction of Fe(II) with superoxide, by reacting Fe(I) with O_2, or by the one-electron electrochemical reduction of the Fe(II) dioxygen complex. Spectroscopic data indicate a high-spin ferric η^2-peroxide complex (type 16-II).

Such information is important for an understanding of the mechanism of the subsequent net oxygen atom transfer [92,142,146,147], which could involve a ferric oxene [Fe^{III}–O] or any of its equivalents (e.g. $Fe^V = O$. Fe^{IV}–$\dot{O}$, (heme$^{+\cdot}$)$Fe^{IV} = O$), and direct insertion, reaction (25), or a radical process involving hydrogen atom abstraction from the substrate, reaction (26).

$$Fe^{III}O_2^{2-} \xrightarrow[-H_2O]{2H^+} Fe^{III}\text{–}O \xrightarrow{RH} Fe^{III} + ROH \qquad (25)$$

$$Fe^{III}O_2^{2-} \xrightarrow[-OH^-]{H^+} Fe^{III}\text{–}O \xrightarrow{RH} \underset{(Fe^{IV}\text{–}OH)}{Fe^{III}\cdots OH} + R\cdot \qquad (26)$$

The *trans* thiolate ligand is probably critical, although its role has not been elucidated; the model systems lack the thiolate ligand and are not active for oxygenation of hydrocarbons [146].

The $Fe^{III}-O$ or $Fe^{V}=O$ species from $Fe^{III}O_2^{2-}$ are, in a formal electron counting sense, equivalent to compounds I of peroxidases and catalases (Fe^{III} enzymes that utilize H_2O_2); their one-electron reduction gives formally Fe^{IV} porphyrins (analogous to compounds II) that correspond to the carbene structures discussed earlier ($Fe^{II} \leftarrow :CR_1R_2 \leftrightarrow Fe^{IV}=CR_1R_2$). Studies on the carbenes should contribute significantly to an understanding of enzymic oxidation involving O_2 or H_2O_2 [148,149].

F. THE μ-LINKED DIMERS

Although some mention of the μ-oxo dimers was made in preceding sections, the diversity of this type of bonding warrants more detailed discussion.

Examples of the three types of μ-oxo dimers found in porphyrin chemistry are illustrated schematically in Fig. 20. The structure shown in 20(a) has been definitely established for the porphyrin complexes of iron [150,151], scandium [151,152] and aluminum [153]. In the case of the paramagnetic iron complexes, antiferromagnetic coupling is observed between the two high spin Fe^{III} nuclei via the nearly linear oxo linkage [68,154,155]. The complexes of Sc^{III} and Al^{III} are of course diamagnetic.

The structures depicted in Fig. 20(b) are represented by the porphyrin complexes of molybdenum [156–158], tungsten [158] and rhenium [158]. The X-ray crystal structure determined for $[Mo(TPP)O]_2O$ [157] is shown in Fig. 21. The five atom unit $O=Mo-O-Mo=O$ is nearly linear with the molybdenum ion being slightly (0.09 Å) displaced from the plane of the four porphyrin nitrogens in the direction of the terminal oxo ligand. Although structural data are not available for either the tungsten or rhenium analogs, similar geometries are assumed on the basis of other spectroscopic properties [68].

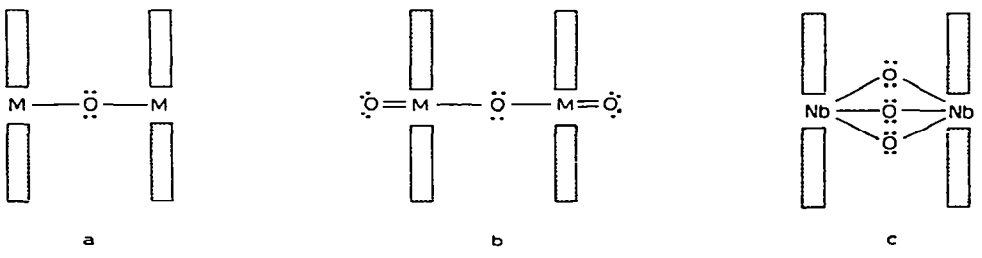

Fig. 20. Examples of μ-oxo complexes.

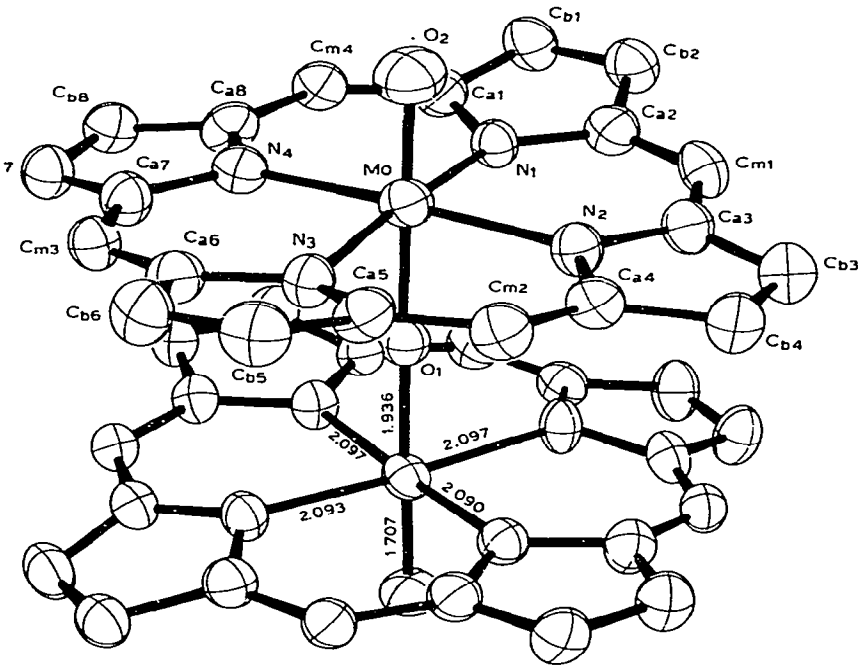

ɜ. 21. Computer drawing of the molecule $[Mo(TPP)O]_2O$ from ref. 157.

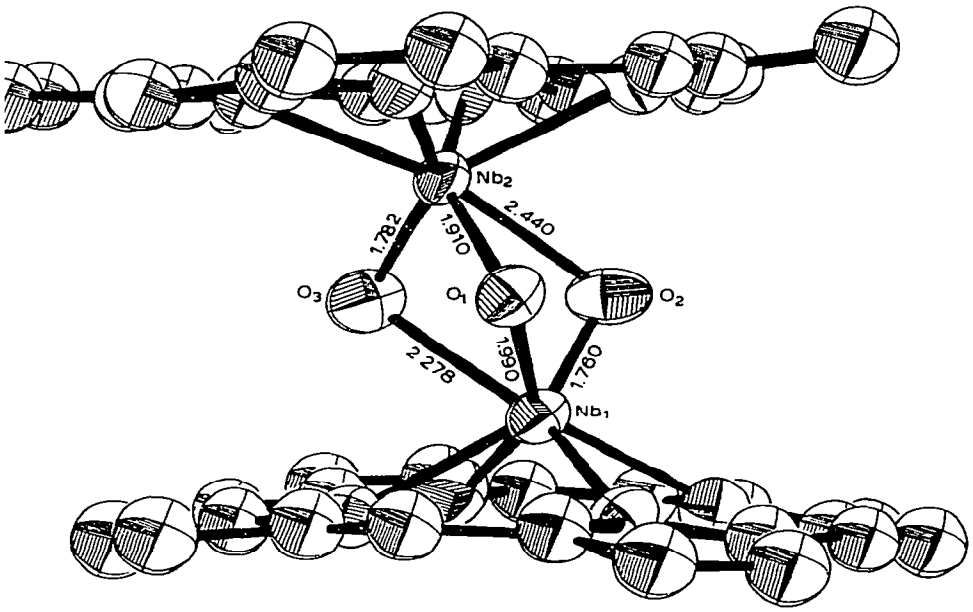

. 22. Computer drawing of the molecule $[Nb(TPP)]_2O_3$ from ref. 157.

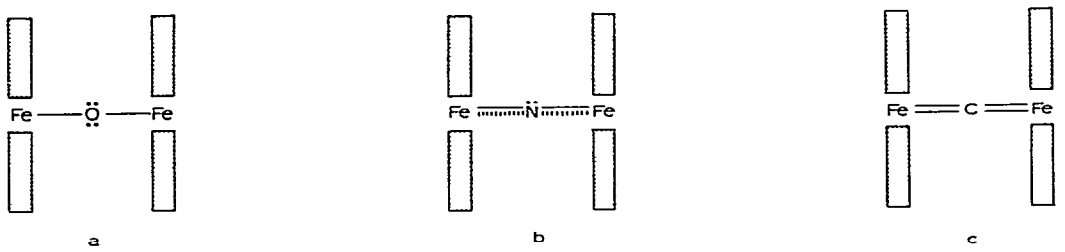

Fig. 23. Schematic representation of (a) μ-oxo, (b) μ-nitrido and (c) μ-carbido complexes.

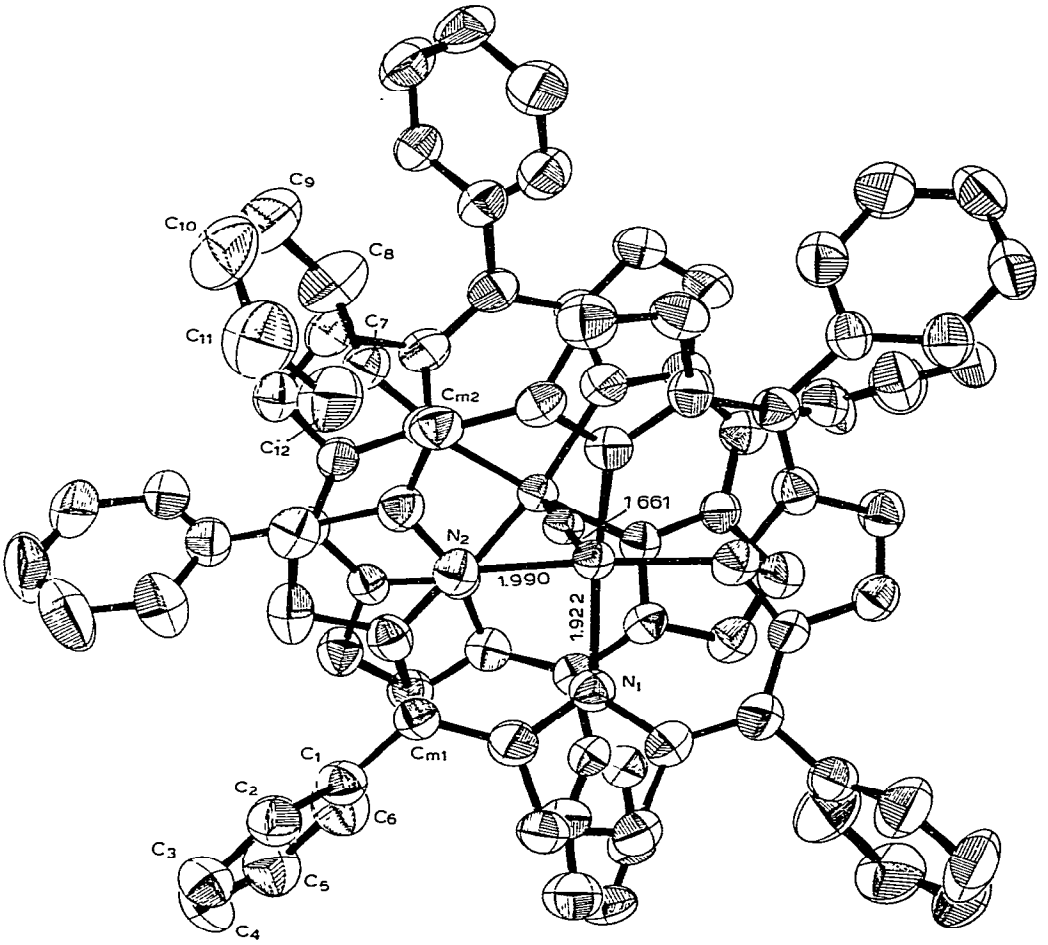

Fig. 24. Computer drawing of the molecule $[Fe(TPP)]_2N$ from ref. 160.

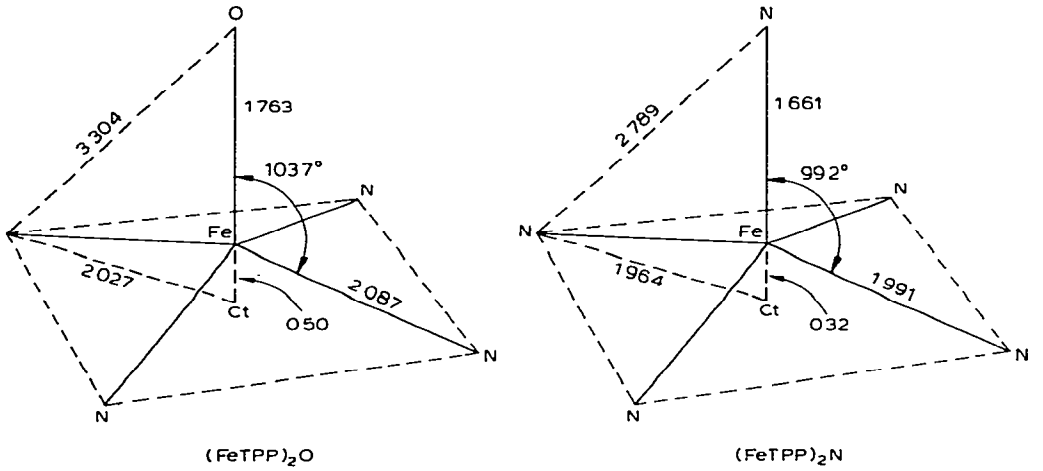

ig. 25. Comparison of coordination geometries for $[Fe(TPP)]_2O$ and $[Fe(TPP)]_2N$ from ref. 50.

The structure of the niobium derivative proved to be quite different in iat all three oxo ligands are in bridging positions between the porphyrin lanes (see Fig. 20(c)). The molecular structure, as determined by X-ray rystallography for $[Nb(TPP)]_2O_3$ [137–157], is shown in Fig. 22. The iobium atom is seven coordinate as determined by the square planar base f porphyrin nitrogens and the trigonal-planar cap of oxo ligands. The three gand planes, consisting of the two porphyrin systems and the one tri-oxo nit, are nearly parallel to each other. The six individual niobium oxygen onds are definitely inequivalent, consisting of one short (ca. 1.77 Å), one ıtermediate (ca. 1.94 Å) and one long (ca. 2.35 Å) to each individual iobium atom. The two slightly inequivalent niobium atoms are displaced pproximately 1.0 Å from the plane of the four porphyrin nitrogens and .35 Å from the plane of the oxo ligands.

In addition to the μ-oxo linkage, recent reports of the μ-nitrido and -carbido bridged iron porphyrins $[Fe(TPP)]_2N$ [159,160] and $[Fe(TPP)]_2C$ 10] respectively, have appeared in the literature. The schematic representa- on of these structures is illustrated in Fig. 23, and the molecular structure f $[Fe(TPP)]_2N$ is presented in Fig. 24. The coordination geometries of $Fe(TPP)]_2O$ and $[Fe(TPP)]_2N$ are compared in Fig. 25. Significant dif- erences are the shorter bridging Fe–N distances compared with the corre- ponding Fe–O distances (consistent with the multiple bond character epicted in Figure 23(b)), and the smaller displacements of the Fe atom from ıe plane of the porphyrin nitrogens toward the bridging ligand in the itrido-complex relative to the oxo-complex. The oxidation state of the Fe

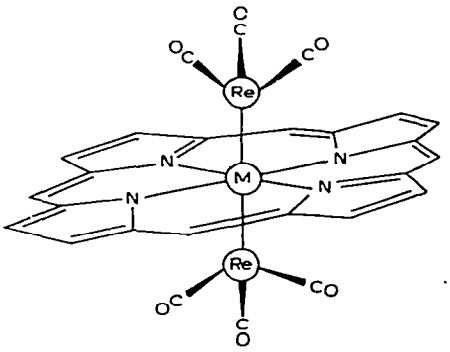

Fig. 26. Schematic representation of the metal–metal bonding in porphyrin complexes.

atoms in the μ-oxo complex is formally +3, with antiferromagnetic coupling ($J = 309$ cm^{-1}) of the two $S = 5/2$ centres producing a temperature dependent magnetic moment. The oxidation state of iron in the μ-nitrido complex is not as clear. The formal oxidation state is $+3\frac{1}{2}$ but the temperature independence of the magnetic moment ($\mu = 2.04$ BM/oligomer) does not allow the unambiguous assignment of spin states for the individual iron

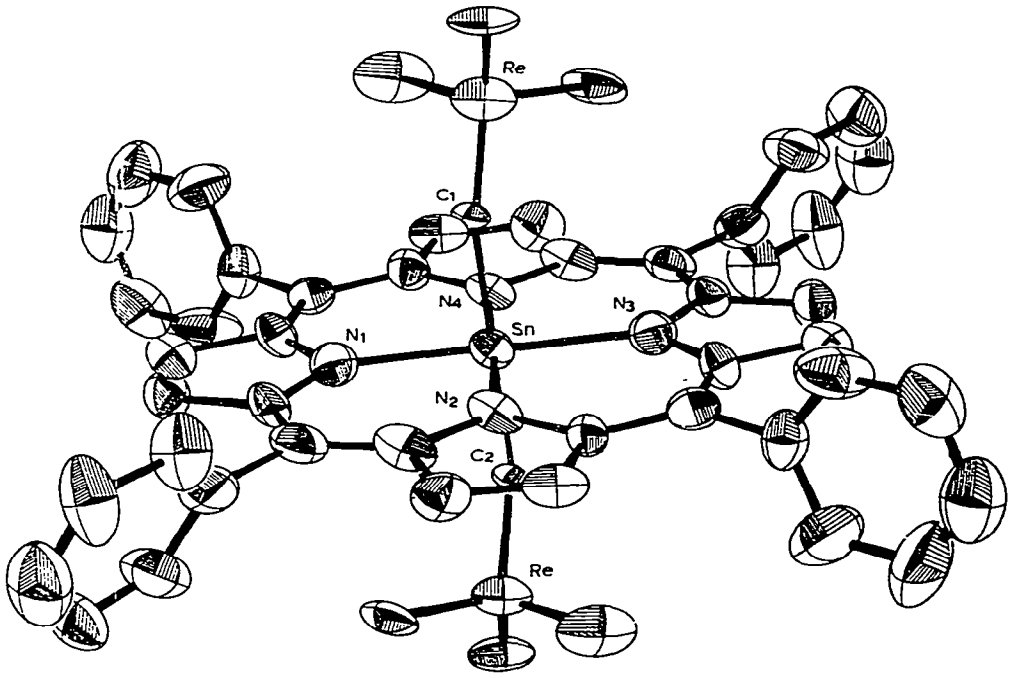

Fig. 27. Computer drawing of the molecule Sn(TPP)[CRe(CO)$_3$]$_2$ from ref. 162.

atoms. Of the two resonance structures possible for the μ-carbido complex

$$(P)Fe^{IV} = C = Fe^{IV}(P) \rightleftharpoons (P)Fe^{II} \leftarrow :C: \rightarrow Fe^{II}(P) \quad (27)$$

the formalism on the right hand side corresponding to divalent iron is more in agreement with the results of various spectroscopic methods. Like the carbenes mentioned in Section C(iii), this complex is diamagnetic.

G. METAL–METAL BONDING

Several porphyrin species with bonding between the porphyrin metal and the metal of a non-porphyrin complex are illustrated in Fig. 26. In these compounds, the central metal is coordinated by two $Re(CO)_3$ ligands in a *trans* configuration giving complexes of the general formula $M(TPP)[Re(CO)_3]_2$, where M = Sn, Zn, Mg and Co [161]. The synthesis of these trinuclear compounds is achieved according to the reactions

$$M(TPP)X_2 + Re_2(CO)_{10} \rightarrow M(TPP)[Re(CO)_3]_2 \quad (28.1)$$

$$M(TPP) + Re_2(CO)_{10} \rightarrow M(TPP)[Re(CO)_3]_2 \quad (28.2)$$

where eqn. 28.1 illustrates the procedure for the tin derivative and eqn. 28.2 that for the divalent zinc, magnesium and cobalt complexes. The nature of the $Re(CO)_3$ ligand remains unclear. In the mono- and dinuclear complexes $[Re(CO)_3]H(TPP)$ [30] and $[Re(CO)_3]_2(TPP)$ [33] discussed earlier, the $Re(CO)_3$ unit appears, at least formally, as $Re(CO)_3^+$ coordinated by three porphyrin nitrogens. In the trinuclear complex $Sn(TPP)[Re(CO)_3]_2$, a formally uninegative $Re(CO)_3^-$ would be necessary to electronically balance a tetravalent Sn^{IV}. However, a neutral $Re(CO)_3$ unit would best describe the bonding in the divalent Zn, Mg and Co complexes. Interestingly, somewhat milder reaction conditions than those employed in the synthesis of the metal–metal bonded trinuclear complex $Sn(TPP)[Re(CO)_3]_2$ result in formation of the bis-(μ-carbidotricarbonyl rhenium) complex $Sn(TPP)[CRe(CO)_3]_2$ [162], the crystal structure of which is shown in Fig. 27. This structure features a carbon atom in a bridging position between the tin and rhenium atoms. The axial bonding can be formally depicted as

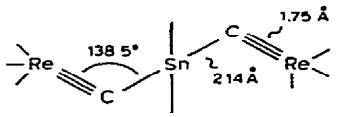

with a carbyne-like bond between the μ-carbido carbon and rhenium.

Several porphyrin dimers involving metal–metal bonds have appeared in the literature, as illustrated in Fig. 28. The ruthenium dimer, $[Ru(OEP)]_2$ [163], forms when a solid sample of the bis-pyridine complex, $Ru(OEP)(Py)_2$ is heated to 220°C under vacuum. The corresponding rhodium complex,

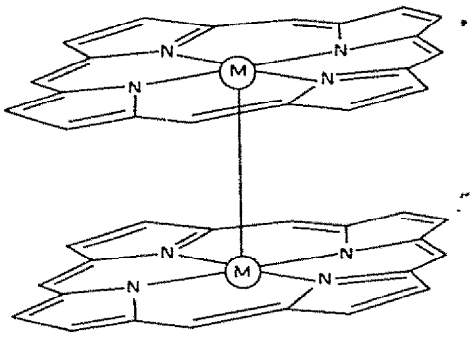

Fig. 28. Porphyrin dimers containing metal–metal bonds.

$[Rh(OEP)]_2$ [129,164], is made from the hydrido complex Rh(OEP)H by either simply dissolving the latter in benzene [164] or by photolysis in toluene [129]

$$Rh(OEP)H \xrightarrow{\text{Benzene}} [Rh(OEP)]_2 + H_2 \quad (29.1)$$

$$Rh(OEP)H \xrightarrow[\text{Toluene}]{h\nu} [Rh(OEP)]_2 + H_2 \quad (29.2)$$

The rhodium dimer reacts with NO at room temperature or O_2 at $-80°C$ to form Rh(OEP)NO and $Rh(OEP)O_2$ respectively [129].

ACKNOWLEDGEMENTS

This work was supported by grants from the Canadian Natural Sciences and Engineering Research Council and the United States National Institutes of Health (AM 17989) and is a contribution from the Bioinorganic Chemistry Group.

REFERENCES

1 (a) D. Dolphin (Ed.), The Porphyrins, Vols. I–VII, Academic Press, New York-San Francisco-London, 1978–79.
(b) K.M. Smith (Ed.), Porphyrins and Metalloporphyrins, Elsevier, Amsterdam-Oxford-New York, 1975.
2 E. Antonini and M. Brunori, Hemoglobin and Myoglobin in their Reactions with Ligands, North-Holland, Amsterdam, 1971.
3 See, for example, Adv. Chem. Ser., 191 (1980).
4 J.P. Collman, P. Denisevich, Y. Konai, M. Marrocco, C. Koval and F.C. Anson. J. Am. Chem. Soc., 102 (1980) 6027.
5 C.R. Wolf, D. Mansuy, W. Nastainczyk, G. Deutschmann and V. Ullrich, Mol. Pharmacol., 13 (1977) 698.

6 B.B. Wayland, L.F. Mehne and J. Swartz, J. Am. Chem. Soc., 100 (1978) 2379.
7 B.B. Wayland, J.V. Minkiewicz and M.E. Abd-Elmageed, J. Am. Chem. Soc., 96 (1974) 2795.
8 G.R. Eaton and S.S. Eaton, J. Am. Chem. Soc., 97 (1975) 235.
9 M. Rougée and D. Brault, Biochem. Biophys. Res. Commun., 55 (1973) 1364.
10 G.W. Sovocool, F.R. Hopf and D.G. Whitten, J. Am. Chem. Soc., 94 (1972) 4350.
11 A. Antipas, J.W. Buchler, M. Gouterman and P.D. Smith, J. Am. Chem. Soc., 100 (1978) 3015.
12 B.C. Chow and I.A. Cohen, Bioinorg. Chem., 1 (1971) 57.
13 R.G. Little and J.A. Ibers, J. Am. Chem. Soc., 95 (1973) 8583.
14 S.S. Eaton, G.R. Eaton and R.H. Holm, J. Organomet. Chem., 39 (1972) 179.
15 J.J. Bonnet, S.S. Eaton, G.R. Eaton, R.H. Holm and J.A. Ibers, J. Am. Chem. Soc., 95 (1973) 2141.
16 J.W. Buchler and K. Rohbock, J. Organomet. Chem., 65 (1974) 223.
17 J.O. Alben, W.H. Fuchsman, C.A. Beaudreau and W.S. Caughey, Biochemistry, 7 (1968) 624.
18 J.W. Faller, C.C. Chen and C.J. Malerich, J. Inorg. Biochem., 11 (1979) 151.
19 J.P. Collman, J.I. Brauman and K.M. Doxsee, Proc. Natl. Acad. Sci. U.S.A., 76 (1979) 6035.
20 E.A. Padlan and W.E. Love, J. Biol. Chem., 249 (1974) 4067.
21 J.C. Norvell, A.C. Nunes and B.P. Schoenborn, Science, 190 (1975) 568.
22 E.J. Heidner, R.C. Ladner and M.F. Perutz, J. Mol. Biol., 104 (1976) 707.
23 M.W. Makinen, R.A. Houtchens and W.S. Caughey, Proc. Natl. Acad. Sci. U.S.A., 76 (1979) 6042.
24 J.M. Baldwin, J. Mol. Biol., 136 (1980) 103.
25 J.W. Buchler, W. Kokisch and P.D. Smith, Struct. Bonding (Berlin), 34 (1978) 1.
26 T. Diebold, M. Schappacher, B. Chevrier and R. Weiss, J. Chem. Soc., Chem. Commun., (1979) 693.
27 I.A. Cohen and B.C. Chow, Inorg. Chem., 13 (1974) 488.
28 H. Ogoshi, J.-I. Setsune and Z. Yoshida, J. Organomet. Chem., 159 (1978) 317.
29 S.-M. Peng and J.A. Ibers, J. Am. Chem. Soc., 98 (1976) 8032.
30 D. Ostfeld, M. Tsutsui, C.P. Hrung and D.C. Conway, J. Coord. Chem., 2 (1972) 101.
31 M. Tsutsui and C.P. Hrung, J. Coord. Chem., 3 (1973) 193.
32 D. Ostfeld, M. Tsutsui, C.P. Hrung and D.C. Conway, J. Am. Chem. Soc., 93 (1971) 2548.
33 M.Tsutsui, C.P. Hrung, D. Ostfeld, T.S. Srivastava, D.L. Cullen and E.F. Meyer Jr., J. Am. Chem. Soc., 97 (1975) 3952.
34 M. Tsutsui and C.P. Hrung, J. Am. Chem. Soc., 96 (1974) 2638.
35 M. Tsutsui and C.P. Hrung, Chem. Lett., (1973) 941.
36 D. Mansuy, J.P. Battioni and J.-C. Chottard, J. Am. Chem. Soc., 100 (1978) 4311.
37 J.W. Buchler, W. Kokisch, P.D. Smith and B. Tonn, Z. Naturforsch. B, 33 (1978) 1371.
38 P.D. Smith, D. Dolphin and B.R. James, J. Organomet. Chem., 208 (1981) 239.
39 D. Mansuy, M. Lange, J.-C. Chottard, P. Guérin, P. Morlière, D. Brault and M. Rougée, J. Chem. Soc., Chem. Commun., (1977) 648.
40 D. Mansuy, Pure Appl. Chem., 52 (1980) 681.
41 D. Mansuy, M. Lange, J.-C. Chottard, J.-F. Bartoli, B. Chevrier and R. Weiss, Angew. Chem. Int. Ed. Engl., 17 (1978) 781.
42 D. Mansuy, M. Lange and J.-C. Chottard, J. Am. Chem. Soc., 100 (1978) 4311.
43 D. Mansuy, J.-P. Battioni, J.-C. Chottard and V. Ullrich, J. Am. Chem. Soc., 101 (1979) 3971.

44 A. Takenaka, Y. Sasada, T. Omura, H. Ogoshi and Z.-I. Yoshida, J. Chem. Soc., Chem. Commun., (1973) 792.
45 S. Silvers, T. Bergeman and W. Klemperer, J. Chem. Phys., 52 (1970) 4385.
46 T. Ziegler and A. Rauk, Inorg. Chem., 18 (1979) 1755.
47 M. Herberhold, P.D. Smith and H.G. Alt, J. Organomet. Chem., 191 (1980) 79.
48 W. Kirmse in A.T. Blomquist (Ed.), Organic Chemistry, A Series of Monographs, vol. 1, Academic Press, New York, 1964.
49 E.O. Fischer and A. Maasböl, Angew. Chem. Int. Ed. Engl., 3 (1964) 580.
50 P.G. Lenhart and D.C. Hodgkin, Nature (London), 192 (1961) 937.
51 B. Zagalak and W. Friedrich (Eds.), Proc. Third European Symposium on Vitamin B_{12} and Intrinsic Factor, W. de Gruyter, Berlin, 1979.
52 D.A. Clarke, D. Dolphin, R. Grigg, A.W. Johnson and H.A. Pinnock, J. Chem. Soc. C, (1968) 881.
53 W.S. Caughey, C.H. Barlow, D.H. O'Keefe and M.C. O'Toole. Ann. N.Y. Acad. Sci., 206 (1973) 296.
54 A.M. Abeysekera, R. Grigg, J. Trocha-Grimshaw and V. Viswanatha, J. Chem. Soc. Perkin I, (1977) 1395.
55 H.J. Callot and E. Schaeffer, J. Organomet. Chem., 145 (1978) 91.
56 H. Ogoshi, J.-I. Setsune, Y. Nanbo and Z. Yoshida, J. Organomet. Chem., 159 (1978) 329.
57 H. Ogoshi, E.-I. Watanabe, N. Koketzu and Z. Yoshida, J. Chem. Soc., Chem. Commun., (1974) 943.
58 H. Ogoshi, T. Omura and Z. Yoshida, J. Am. Chem. Soc., 95 (1973) 1666.
59 P. Ortiz de Montellano, B.A. Mico, H.S. Beilan and K.L. Kunze, in T. Singer and R. Ondarza (Eds.), Molecular Basis of Drug Action, Elsevier, in press.
60 H. Ogoshi, J.-I. Setsune, T. Omura and Z. Yoshida, J. Am. Chem. Soc., 97 (1975) 6461.
61 B.R. James and D.V. Stynes, J. Chem. Soc., Chem. Commun., (1972) 1261.
62 C. Cloutour, D. Lafargue and J.C. Pommier, J. Organomet. Chem., 161 (1978) 327.
63 A.D. Allen and C.V. Senoff, J. Chem. Soc., Chem. Commun., (1965) 621.
64 (a) D. Sellman, Angew. Chem. Int. Ed. Engl., 13 (1974) 639.
(b) J. Chatt, in A.W. Addison, W.R. Cullen, D. Dolphin and B.R. James (Eds.), Biological Aspects of Inorganic Chemistry, Wiley, New York, 1977, p. 229.
(c) A.E. Shilov, in A.W. Addison, W.R. Cullen, D. Dolphin and B.R. James (Eds.), Biological Aspects of Inorganic Chemistry, Wiley, New York, 1977, p. 197.
(d) D.L. Thorn, T.H. Tulip and J.A. Ibers, J. Chem. Soc., Dalton Trans., (1979) 2022, and references therein.
65 S. McCoy and W.S. Caughey, Biochemistry, 9 (1970) 2387.
66 (a) B.R. James, A.W. Addison, M. Cairns, D. Dolphin, N.P. Farrell, D.R. Paulson and S. Walker in M. Tsutsui (Ed.), Fund. Research in Homog. Catal., Vol. 3, Plenum Press, New York, 1979, p. 751.
(b) N. Farrell, D.H. Dolphin and B.R. James, J. Am. Chem. Soc., 100 (1978) 324.
67 J.W. Buchler and P.D. Smith, Angew. Chem., 86 (1974) 820; Angew. Chem. Int. Ed. Engl., 13 (1974) 745.
68 J.W. Buchler, in D. Dolphin (Ed.), The Porphyrins, Vol. I, Academic Press, 1978, p. 390.
69 W.R. Scheidt, K. Hatano, G.A. Rupprecht and P.L. Piciulo, Inorg. Chem., 18 (1979) 292.
70 W.R. Scheidt and M.E. Frisse, J. Am. Chem. Soc., 97 (1975) 18.
71 W.R. Scheidt and J.L. Hoard, J. Am. Chem. Soc., 95 (1973) 8281.
72 J.H. Enemark and R.D. Feltham, Coord. Chem. Rev., 13 (1974) 339.
73 W.R. Scheidt and P.L. Piciulo, J. Am. Chem. Soc., 98 (1976) 1913.

74 J.W. Buchler and P.D. Smith, Chem. Ber., 109 (1976) 1465.
75 J.W. Buchler, 1980, personal communication reporting the synthesis of Mn(OEP)N.
76 A. Antipas, J.W. Buchler, M. Gouterman and P.D. Smith, J. Am. Chem. Soc., 102 (1980) 198.
77 H. Ogoshi, E. Watanabe, Z. Yoshida, J. Kincaid and J. Nakamoto, J. Am. Chem. Soc., 95 (1973) 2845.
78 H. Ogoshi and Z. Yoshida, Chem. Lett., (1972) 1235.
79 F. Basolo, B.M. Hoffman and J.A. Ibers, Acc. Chem. Res., 8 (1975) 384.
80 R.W. Erskine and B.O. Field, Struct. Bonding, 28 (1976) 1.
81 G. McLendon and A.E. Martell, Coord. Chem. Rev., 19 (1976) 1.
82 L. Vaska, Acc. Chem. Res., 9 (1976) 175.
83 J.H. Fuhrhop, Angew. Chem. Int. Ed. Engl., 15 (1976) 648.
84 J.P. Collman, Acc. Chem. Res., 10 (1977) 265.
85 J.W. Buchler, Angew. Chem. Int. Ed. Engl., 17 (1978) 407.
86 T.G. Traylor, in E.E. Van Tamelen (Ed.), Bioorganic Chemistry, Vol. IV, Academic Press, New York, 1978, p. 437.
87 B.R. James, in D. Dolphin (Ed.), The Porphyrins, Vol. V, Academic Press, New York, 1978, p. 205.
88 E.I. Ochiai, Bioinorganic Chemistry, An Introduction, Allyn and Bacon, Boston, 1977, Chaps. 6, 7 and 10.
89 R.D. Jones, D.A. Summerville and F. Basolo, Chem. Rev., 79 (1979) 139.
90 C.A. Reed, in H. Sigel (Ed.), Metal Ions in Biological Systems, Vol. 7, Marcel Dekker, New York, 1978, p. 278.
91 J.P. Collman, T.R. Halbert and K.S. Suslick, in T.G. Spiro (Ed.), Metal Ion Activation of Dioxygen, Wiley, New York, 1980, p. 1.
92 M.J. Coon and R.E. White, in T.G. Spiro (Ed.), Metal Ion Activation of Dioxygen, Wiley, New York, 1980, p. 73.
93 J.T. Groves, in T.G. Spiro (Ed.), Metal Ion Activation of Dioxygen, Wiley, New York, 1980, p. 125.
94 J.M. Wood, in T.G. Spiro (Ed.), Metal Ion Activation of Dioxygen, Wiley, New York, 1980, p. 163.
95 B.G. Malström, in T.G. Spiro (Ed.), Metal Ion Activation of Dioxygen, Wiley, New York, 1980, p. 181.
96 G.B. Jameson, F.S. Molinaro, J.A. Ibers, J.P. Collman, J.I. Brauman, E. Rose and K.S. Suslick, J. Am. Chem. Soc., 102 (1980) 3224 and references therein.
97 S.E.V. Phillips, Nature (London), 273 (1978) 247.
98 G.A. Petsko, D. Rose, D. Tsernoghon, M. Ikeda-Saito and T. Yonetani, in P.L. Dutton, J.S. Leigh, Jr. and A. Scarpa (Eds.), Frontiers of Biological Energetics, Academic Press, New York, 1978, p. 1011.
99 C.K. Chang, D. Powell and T.G. Traylor, Croat. Chem. Acta, 49 (1977) 295.
100 D.-H. Chin, G.N. La Mar and A.L. Balch, J. Am. Chem. Soc., 102 (1980) 4344.
101 M.M.L. Chu, C.E. Castro and G.M. Hathoway, Biochemistry, 17 (1978) 481.
102 D.R. Eaton and K.M. Wilson, J. Inorg. Biochem., 10 (1979) 195.
103 J. Billecke, W. Kokisch and J.W. Buchler, J. Am. Chem. Soc., 102 (1980) 3622.
104 J. Almog, J.E. Baldwin and J. Huff, J. Am. Chem. Soc., 97 (1975) 227.
105 J.R. Budge, P.E. Ellis, R.D. Jones, J.E. Linard, T. Szymanski, F. Basolo, J.E. Baldwin and R.L. Dyer, J. Am. Chem. Soc., 101 (1979) 4762.
106 J.R. Budge, P.E. Ellis, R.D. Jones, J.E. Linard, F. Basolo, J.E. Baldwin and R.L. Dyer, J. Am. Chem. Soc., 101 (1979) 4760.

107 A.R. Battersby and A.D. Hamilton, J. Chem. Soc., Chem. Commun., (1980) 117.
108 M. Momenteau and B. Loock, J. Mol. Catal., 7 (1980) 315.
109 O. Leal, D.L. Anderson, R.G. Bowman, F. Basolo and R.L. Burwell, J. Am. Chem. Soc., 97 (1975) 5125.
110 E. Bayer and G. Holzbach, Angew. Chem. Int. Ed. Engl., 16 (1977) 117.
111 A.H. Corwin and S.D. Bruck, J. Am. Chem. Soc., 80 (1958) 4736.
112 C.K. Chang and T.G. Traylor, J. Am. Chem. Soc., 95 (1973) 5810.
113 T.G. Traylor, C.K. Chang, J. Geibel, A. Berzinis, T. Mincey and J. Cannon, J. Am. Chem. Soc., 101 (1979) 6716.
114 D.A. Summerville, R.D. Jones. B.M. Hoffman and F. Basolo, J. Chem. Educ., 56 (1979) 157.
115 R.S. Drago and B.B. Corden, Acc. Chem. Res., 13 (1980) 353.
116 W.H. Fuchsman, C.H. Barlow, W.J. Wallace and W.S. Caughey, Biochem. Biophys. Res. Commun., 61 (1974) 585.
117 J.-M. Latour, J.-C. Marchon and M. Nakajima, J. Am. Chem. Soc., 101 (1979) 3974.
118 J.-C. Marchon, J.-M. Latour and C.J. Boreham, J. Mol. Catal., 7 (1980) 227.
119 J.-C. Marchon, 1980, private communication.
120 R. Guilard, M. Fontesse, P. Fournari, C. Lecomte and J. Protas, J. Chem. Soc., Chem. Commun., (1976) 161.
121 B. Chevrier, T. Diebold and R. Weiss, Inorg. Chim. Acta, 19 (1976) L57.
122 R.D. Jones, D.A. Summerville and F. Basolo, J. Am. Chem. Soc., 100 (1978) 4416.
123 B.F. Hoffman, T. Szymanski, T.G. Brown and F. Basolo, J. Am. Chem. Soc., 100 (1978) 7253.
124 A. Dedieu and H.-M. Rohmer, J. Am. Chem. Soc., 99 (1977) 8050.
125 D.A. Summerville, T.W. Cape, E.D. Johnson and F. Basolo, Inorg. Chem., 17 (1978) 3297.
126 M. Cairns, D. Dolphin and B.R. James, 1978, unpublished data.
127 B.R. James and D.W. Smith, 62nd Canadian Chem. Conf., Vancouver, 1979, The Chemical Institute of Canada, Abstract IN-44.
128 B.R. James and D.V. Stynes, J. Am. Chem. Soc., 94 (1972) 6225.
129 B.B. Wayland and A.R. Newman, J. Am. Chem. Soc., 101 (1979) 6472.
130 D.V. Stynes, H.C. Stynes, J.A. Ibers and B.R. James, J. Am. Chem. Soc., 95 (1973) 1142.
131 F.A. Walker, J. Am. Chem. Soc., 92 (1970) 4235.
132 F.A. Walker, J. Am. Chem. Soc., 95 (1973) 1154.
133 E. Ochiai, Inorg. Nucl. Chem. Lett., 10 (1974) 453.
134 D.-H. Chin, J. Del Gaudio, G.N. La Mar and A.L. Balch, J. Am. Chem. Soc., 99 (1977) 5486.
135 D.-H. Chin, G.N. La Mar and A.L. Balch, J. Am. Chem. Soc., 102 (1980) 4344.
136 J.E. Baldwin and J. Huff, J. Am. Chem. Soc., 95 (1973) 5757.
137 C. Lecomte, J. Protas, R. Guilard, B. Fliniaux and P. Fournari, J. Chem. Soc., Dalton Trans., (1979) 1306.
138 J.W. Buchler and P.D. Smith, Angew. Chem., Int. Ed. Engl., 13 (1974) 341.
139 H. Ledon, M. Bonnet and J.-Y. Lallemard, J. Chem. Soc., Chem. Commun., (1979) 702.
140 H. Ledon and M. Bonnet, J. Mol. Catal., 7 (1980) 309; Abstr., 1st Int. Symp. O_2 Activation and Selective Oxidations Catalyzed by Transition Metals, Bendor, 1979.
141 V. Ullrich, J. Mol. Catal., 7 (1980) 159.
142 D. Dolphin, A.W. Addison, M. Cairns, R.K. DiNello, N.P. Farrell, B.R. James, D.R. Paulson and H.C. Welborn, Int. J. Quantum Chem., 16 (1979) 311.
143 D. Dolphin, B.R. James and H.C. Welborn, J. Mol. Catal., 7 (1980) 201.

144 E. McCandlish, A.R. Miksztal, M. Nappa, A.Q. Sprenger, J.S. Valentine, J.D. Stong and T.G. Sprio, J. Am. Chem. Soc., 102 (1980) 4268.
145 C.A. Reed, T. Mashiko, W.R. Scheidt and R. Haller, 1st Int. Symp. O_2 Activation and Selective Oxidations Catalyzed by Transition Metals, Bendor, 1979, Poster Abstract.
146 D. Dolphin, B.R. James and C.H. Welborn, J. Am. Chem. Soc., 103 (1981).
147 J.T. Groves, T.E. Nemo and R.S. Myers, J. Am. Chem. Soc., 101 (1979) 1032.
148 D. Mansuy, M. Lange and J.-C. Chottard, J. Am. Chem. Soc., 101 (1979) 6437.
149 D. Mansuy, J.-C. Chottard, M. Lange and J.-P. Battioni, J. Mol. Catal., 7 (1980) 215.
150 A.B. Hoffman, D.M. Collins, V.W. Day, E.B. Fleischer, T.S. Srivastava and J.L. Hoard, J. Am. Chem. Soc., 94 (1972) 3620.
151 J.W. Buchler and H.H. Schneehage, Z. Naturforsch. B, 28 (1973) 433.
152 M. Gouterman, L.K. Hanson, G.-E. Khalil, J.W. Buchler, K. Rohbock and D. Dolphin, J. Am. Chem. Soc., 97 (1975) 3142.
153 J.W. Buchler, L. Puppe and H.H. Schneehage, Justus Liebigs Ann. Chem., 749 (1971) 134.
154 D.H. O'Keefe, C.H. Barlow, G.A. Smythe, W.H. Fuchsman, T.H. Moss, H.R. Lilienthal and W.S. Caughey, Bioinorg. Chem., 5 (1975) 125.
155 H. Leuken, J.W. Buchler and K.L. Lay, Z. Naturforsch. B, 31 (1976) 1596.
156 E.F. Fleischer and T.S. Srivastava, Inorg. Chim. Acta, 5 (1971) 151.
157 J.F. Johnson and W.R. Scheidt, Inorg. Chem., 17 (1978) 1280.
158 J.W. Buchler and K. Rohbock, Inorg. Nucl. Chem. Lett., 8 (1972) 1073.
159 D.A. Summerville and I.A. Cohen, J. Am. Chem. Soc., 98 (1976) 1747.
160 W.R. Scheidt, D.A. Summerville and I.A. Cohen, J. Am. Chem. Soc., 98 (1976) 6623.
161 S. Kato, I. Noda, M. Mizuta and Y. Itoh, Angew. Chem. Int. Ed. Engl., 18 (1979) 82.
162 I. Noda, S. Kato, M. Mizuta, N. Yasuoka and N. Kasai, Angew. Chem. Int. Ed. Engl., 18 (1979) 83.
163 F.R. Hopf, T.P. O'Brien, W.R. Scheidt and D.G. Whitten, J. Am. Chem. Soc., 97 (1975) 277.
164 H. Ogoshi, J. Setsune and Z. Yoshida, J. Am. Chem. Soc., 99 (1977) 3869.
165 J.W. Buchler, G. Eikelmann, L. Puppe, K. Rohbock, H.H. Schneehage and D.D. Weck, Justus Liebigs Ann. Chem., 745 (1971) 135.
166 J.-H. Fuhrhop, Tetrahedron Lett., (1969) 3205.
167 M. Tsutsui, R.A. Velapoldi, K. Suzuki, F. Vohwinkel, M. Ichakawa and T. Koyano, J. Am. Chem. Soc., 91 (1969) 6262.
168 A. Treibs, Ann. Chem., 517 (1935) 172.
169 J.G. Erdman, V.G. Ramsey, W.W. Kalenda and W.E. Hanson, J. Am. Chem. Soc., 78 (1956) 5844.
170 J.W. Buchler, L. Puppe, K. Rohbock and H.H. Schneehage, Chem. Ber., 106 (1973) 2710.